# CHAPTER 11

# DESIGN OPTIMIZATION AND TRADE-OFF CASE STUDY RESULTS

This chapter discusses the design optimization case studies described in Section 8.6. All of the optimization plots in this chapter show normalized optimization variables X1 and X2 as the horizontal axis. -1 and 1 refer to the lower and upper move limits of the optimization variable or variable group. Each variable group is defined at the beginning of each case study. Each optimization search dimension is divided into 10 increments, so there are 11 data points across each horizontal axis. The vertical axis refers to the change (in percent) in the overall assembly rating, namely the weakest total resistance (WTR), mean redundancy ratio (MRR), mean total resistance (MTR), and trade-off ratio (TOR). Explanation of these rating metrics can be found in Chapter 6. The case study geometries and constraint configurations can be found in Chapter 10. In this chapter, the word optimum is to be understood as the optimum within the design spaces, which act as the optimization constraints.

## 11.1 Exactly constrained geometry - Thompson's chair

### 11.1.1 One-dimensional optimization of the height

The purpose of this study is to optimize the height variable. The objective of the optimization is to maximize the WTR rating. The optimized variable is the position of CP7 along the z-axis. This is done by conducting a one-dimensional line search. The optimization variable and move limits are specified in Table 11.1

| | Constraint variables | Line search center point | Line search direction | Move limits |
|---|---|---|---|---|
| **Variable group X1** | CP7 | $[0 \quad 0 \quad 4]$ | $[0 \quad 0 \quad 1]$ | $-1 \leq x_1 \leq 1$ |

**Table 11.1 Optimization variables and search space for Thompson's chair height**

The optimization plot (Figure 11.1) shows that the WTR rating remains unchanged for any height. Although CP7 actively resists the most weakly constrained motion, its resistance value does not change as the height is varied. The reason is that the moment arm length between the screw axis and CP7 does not change along the line search space. The MRR also does not change for any height value because throughout the line search, the linear independence of CP7 to the rest of the constraints is not changed. Total restraint is still maintained. MTR is increased as the chair height is reduced and improved 0.8% at the minimum height of 3 inches. Therefore, a shorter chair has better

resistance to the overall evaluated motion than a higher chair. In general, the closer an object is to a uniform length in all directions the more uniform resistance it has in all directions.

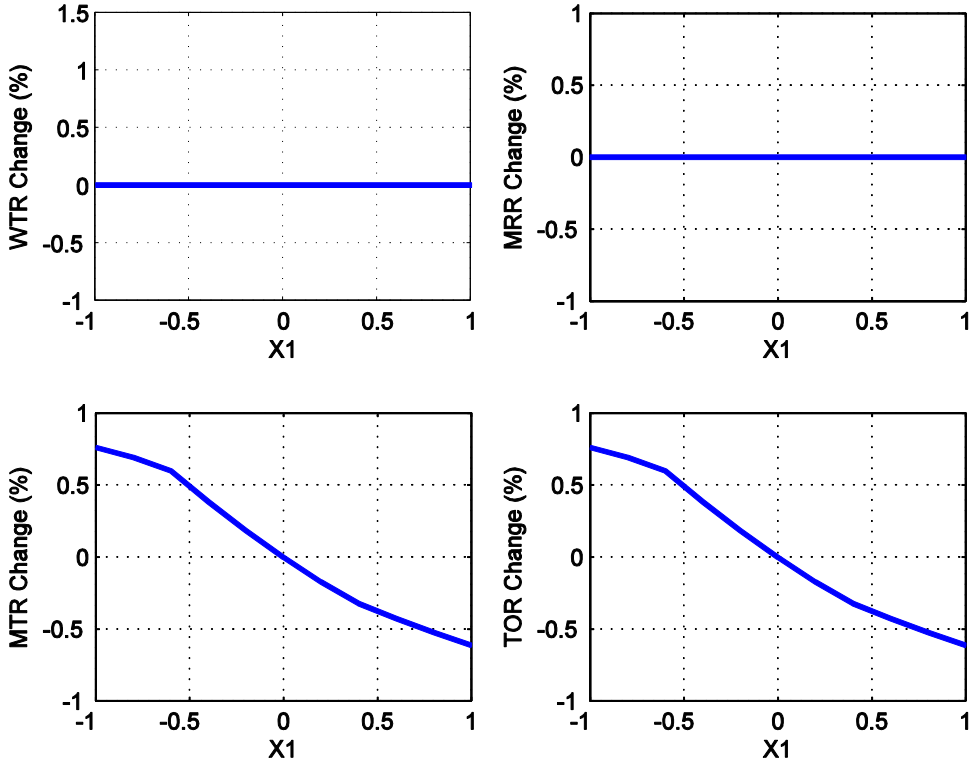


**Figure 11.1 Optimization plot for Thompson's chair height variable**

### 11.1.2 Two-dimensional optimization of the height and trihedral angle

The purpose of this study is to add one more variable to the optimization study in the previous section so as to understand the interaction between the two variables. In this study the trihedral constraint direction is added as an optimization variable. The MATLAB script does not have the capability to vary the angle of all three trihedral point

constraints as one parameter. Therefore, only the orientation of CP2 is optimized. The optimization variables and move limits are specified in Table 11.2. All positive signs in rotation angle refer to the clockwise direction.

| | Constraint variables | Line search center point | Line search direction | Move limits |
|---|---|---|---|---|
| **Variable group X1** | CP7 | $[0 \quad 0 \quad 4]$ | $[0 \quad 0 \quad 1]$ | $-1 \leq x_1 \leq 1$ |
| | **Line search direction** | **Orientation rotation axis** | | **Rotation angle limits** |
| **Variable group X2** | CP2 | $[0 \quad 1 \quad 0]$ | | $-30° \leq \theta_1 \leq 30°$ |

**Table 11.2 Optimization variables and search space for Thompson's chair height and trihedral angle**

The response plot is shown in Figure 11.2. The WTR rating plot shows a discontinuity in some regions of the surface (X2=0.2). When a discontinuity occurs in the response surface plots (WTR), the optimum solution shifts to a different WTR motion. This results in a totally different value range. The WTR plot shows that the assembly is stronger as the angle of CP2 is changed. As the angle of CP2 is changed, the reciprocal motions where CP2 is one of the pivot constraints change. These reciprocal motions are resisted more strongly than in the previous solution. The response surface plots shows no interaction between the two variables. It can be observed that the effect of the angle of CP2 has more effect on the MTR compared to the position of CP7. MTR increases as the orientation of CP2 is closer to the z-axis. The design recommendation then is to rotate CP2 in a clockwise direction and shorten the height of the chair to increase both the WTR and the MTR ratings.

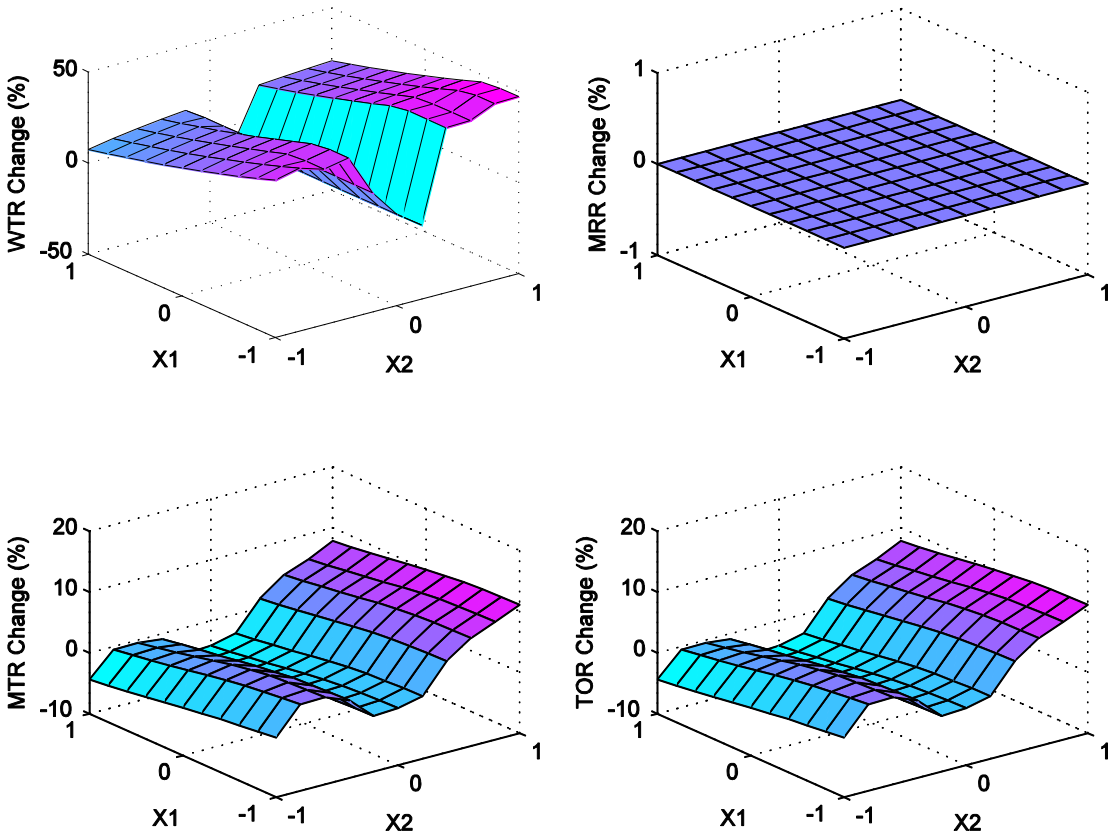


**Figure 11.2 Optimization plot for Thompson's chair height and CP3 angle variable**

## 11.2 Simple 3D shape geometry - generic cube

### 11.2.1 Constraint addition trade-off case study

The purpose of this case study is to gain an understanding of assembly behavior as the number of constraints is increased. Table 10.5 shows the different constraint combinations as the constraints are added.

| Number of constraints | Constraint combination |
|---|---|
| **7** | CP2,CP3,CP4,CP5,CP7,CP10,CP12 |
| **8** | CP1,CP2,CP3,CP4,CP5,CP7,CP10,CP12 |
| **9** | CP1,CP2,CP3,CP4,CP5,CP6,CP7,CP10,CP12 |
| **10** | CP1,CP2,CP3,CP4,CP5,CP7,CP8,CP10,CP11,CP12 |
| **11** | CP1,CP2,CP3,CP4,CP5,CP6,CP7,CP8,CP10,CP11,CP12 |
| **12** | CP1,CP2,CP3,CP4,CP5,CP6,CP7,CP8,CP9,CP10,CP11,CP12 |
| **13** | CP1,CP2,CP3,CP4,CP5,CP6,CP7,CP8,CP9,CP10,CP11,CP12,CP13 |
| **14** | CP1,CP2,CP3,CP4,CP5,CP6,CP7,CP8,CP9,CP10,CP11,CP12,CP13,CP14 |
| **15** | CP1,CP2,CP3,CP4,CP5,CP6,CP7,CP8,CP9,CP10,CP11,CP12,CP13,CP14,CP15 |

**Table 11.3 Cube constraint combinations for different number of constraints**

Table 11.4 and Figure 11.3 show the overall ratings of the assembly as constraints are added by random selection. The WTR and MTR rating increases monotonically as constraints are added. However, the redundancy rating MRR also increases. The redundancy increases at approximately the same rate as the overall resistance quality, yielding an approximately constant trade-off ratio (TOR).

| No. of Constraints | WTR | MRR | MTR | TOR |
|---|---|---|---|---|
| 7 | 0.200 | 1.000 | 0.486 | 0.486 |
| 8 | 0.200 | 1.165 | 0.594 | 0.510 |
| 9 | 0.200 | 1.389 | 0.678 | 0.488 |
| 10 | 0.216 | 1.745 | 0.930 | 0.533 |
| 11 | 0.381 | 1.981 | 0.975 | 0.492 |
| 12 | 0.381 | 2.115 | 1.058 | 0.500 |
| 13 | 0.381 | 2.239 | 1.156 | 0.516 |
| 14 | 0.381 | 2.547 | 1.285 | 0.505 |
| 15 | 0.555 | 2.693 | 1.376 | 0.511 |

**Table 11.4 Overall rating increase as constraints are added**

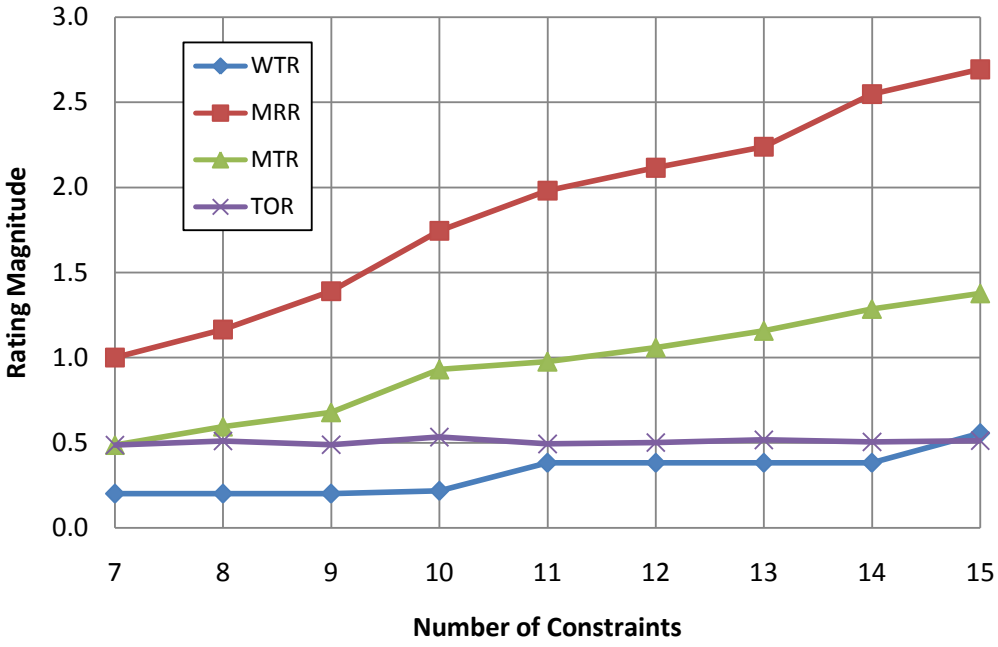


**Figure 11.3 Overall rating increase as constraints are added**

A closer look at the WTR rating increase shows that WTR does not always increase as constraints are added. Because WTR rating is the total resistance for the most weakly constrained motion, it is possible that newly added constraints are not actively resisting the most weakly constrained motion. This happens when the new constraint is linearly dependent to the pivot constraint set of the most weakly constrained motion or when the line-of-action causes a loss of contact from the new constraint. In this case, it does not provide additional resistance to the most weakly constrained motion, and hence no increase is observed in the WTR rating. Furthermore, by observing cases when WTR increases after the addition of constraints, better candidate constraints that are more critical to the most weakly constrained motion can be identified. When this is the concern, this procedure can be used to select better candidates among a few possible

constraints. For example, the increase of the WTR rating from 9 constraints to 10 constraints is achieved by CP11, from 10 constraints to 11 constraints by CP6, and from 14 constraints to 15 constraints by CP15.

### 11.2.2 Constraint reduction trade-off case study

The purpose of this case study is to gain an understanding of assembly behavior as constraints are reduced. Reduction of constraints aims to reduce redundancy in assembly DOF removal, while keeping the negative impact on assembly resistance quality minimal. This is where the rating metric TOR becomes useful. TOR is the ratio between MTR and MRR. Removing constraints can increase the TOR when the constraint to be removed is selected optimally.

Figure 11.4 shows a plot of the rating change as each constraint is removed one at a time. The horizontal axis refers to the constraint index. This refers to individual constraints regardless of their type. This index can be cross-referenced to a particular constraint. This figure is useful to identify which constraints are critical to the resistance of the assembly configuration as well as the ones that are responsible for adding redundancy. Constraints that have a negative impact on the WTR or MTR rating when removed are the ones critical to providing resistance (CP3, CP8, and CP11). Constraints that have a negative impact on MRR when removed are the ones responsible for adding redundancy (CP3, CP8). Constraints that have a negative impact on TOR when removed are ones that add more strength than redundancy. It is desirable to keep these constraints. Constraints that have a positive impact on TOR when removed are ones that add more

redundancy than strength. These constraints are the better candidates to remove (CP6, CP8, CP10, and CP14). The goal is then is to identify constraints that yield the maximum increase in TOR and remove them to optimize assembly in the context of constraint reduction. In this case, CP3 is the most critical constraint to the resistance quality. In fact, when CP3 is removed, the assembly loses total restraint. CP6 is identified as the best candidate to increase TOR when removed.

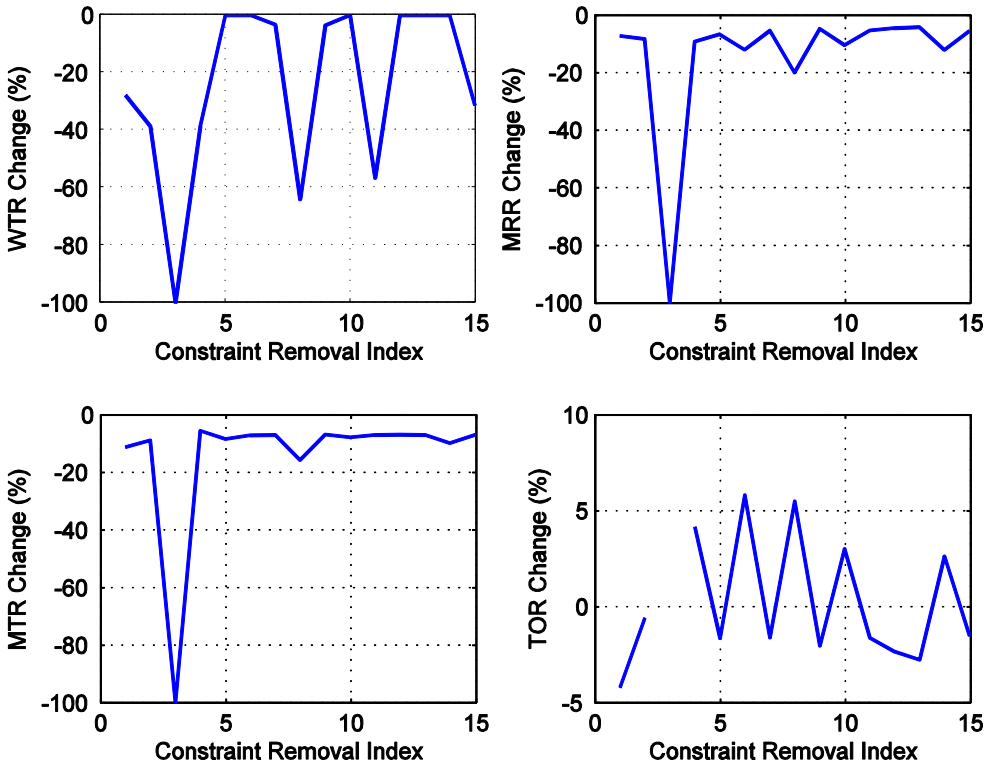


**Figure 11.4 Rating change due to constraint removal (one at a time)**

When the goal of the designer is to remove more than one constraint, a scheme to pick combinations of two constraints is used. Figure 11.5 shows a plot where two

constraints are removed at one time. The x-axis signifies the index of the scheme of different combinations. In this case, there are a total of 105 different combinations of 2 constraints to remove from 15 constraints.

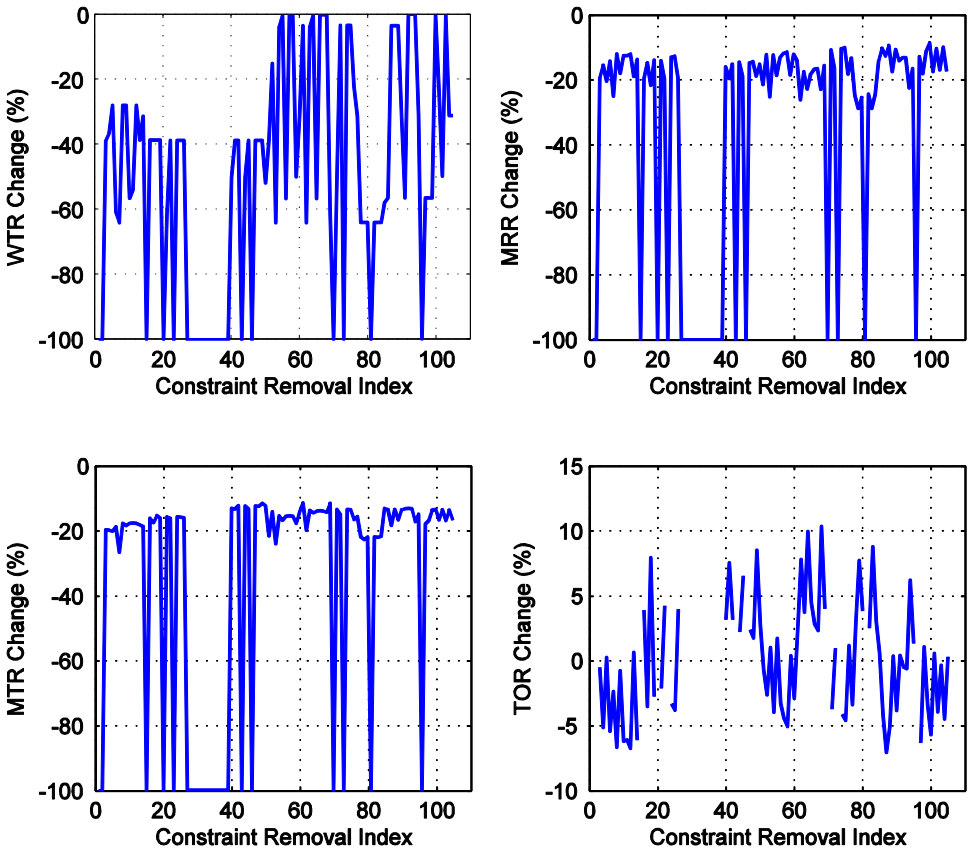


**Figure 11.5 Rating change due to constraint removal (two at a time)**

In the plot, there are more cases where the assembly loses a significant resistance quality. This is possible because as more constraints are removed, the possibility for an assembly to lose its ability to resist motion is significantly higher. In some cases, the assembly loses total restraint altogether. It is very important to note constraint

combinations that are critical in maintaining total restraint. In this case, removing constraint combination #68 yields the maximum possible TOR increase. This constraint combination index cross-references to constraints CP6 and CP14. In the rating matrix, there is a motion that is resisted by CP6 and CP14, but not by any other constraints. Once these constraints are eliminated, the motion becomes unconstrained.

The procedure explained above can be further extended to remove more constraints at a time up to the maximum possible number. In this case study, it is possible to remove up to 8 constraints at a time. It is impossible to remove more than 8 constraints because the number of constraints remaining will be below the required seven point constraint requirement to achieve total restraint. Table 11.5 and Figure 11.6 show the overall rating changes as more constraints are removed.

| No of Constraints removed | Maximum Possible TOR increase (%) | WTR | MRR | MTR | Removed Constraints | | | | | | | |
|---|---|---|---|---|---|---|---|---|---|---|---|---|
| 0 | 0.0 | 0.555 | 2.693 | 1.376 | | | | | | | | |
| 1 | 5.8 | 0.555 | 2.370 | 1.282 | 6 | | | | | | | |
| 2 | 10.4 | 0.555 | 2.091 | 1.180 | 6 | 14 | | | | | | |
| 3 | 15.5 | 0.555 | 1.820 | 1.075 | 6 | 14 | 10 | | | | | |
| 4 | 19.0 | 0.340 | 1.555 | 0.945 | 6 | 14 | 10 | 1 | | | | |
| 5 | 17.2 | 0.340 | 1.393 | 0.834 | 6 | 14 | 10 | 1 | 2 | | | |
| 6 | 17.2 | 0.340 | 1.262 | 0.756 | 6 | 14 | 10 | 7 | 2 | 4 | | |
| 7 | 15.0 | 0.340 | 1.131 | 0.665 | 6 | 14 | 10 | 7 | 2 | 4 | 12 | |
| 8 | 11.9 | 0.340 | 1.000 | 0.572 | 6 | 14 | 10 | 7 | 2 | 4 | 12 | 13 |

**Table 11.5 Overall rating change as more constraints are removed**

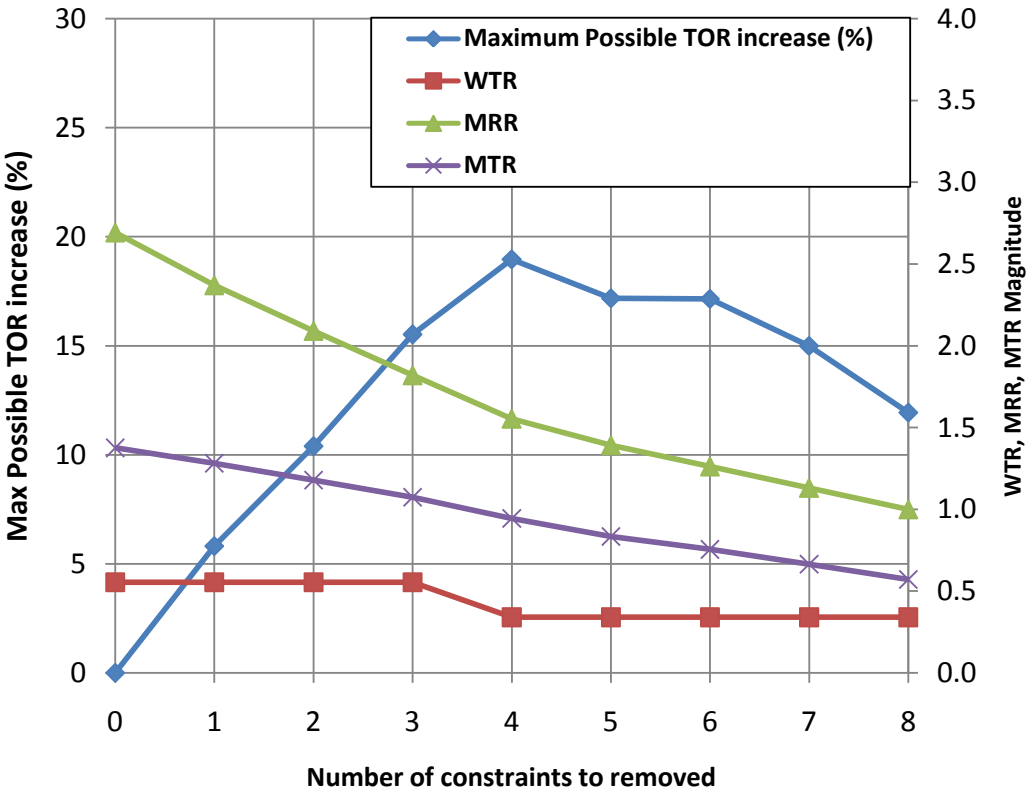


**Figure 11.6 Overall rating change as constraints are removed**

Note that there are two vertical axes on the plot. The left side vertical axis is for the TOR increase (%), and the right side is for the assembly ratings WTR, MRR, and MTR ratings. The first set of results is the baseline results (zero constraint removed, zero TOR increase). It can be observed that as more constraints are removed at a time, the assembly ratings WTR, MRR, and MTR monotonically decrease. MRR reduces to 1.0, which is expected for an exactly constrained assembly (7 constraints). The constraints to remove are selected optimally in a way that minimizes the reduction in MTR and maximizes the reduction in MRR or in other words, maximizing TOR increase. There might be multiple possibilities to increase TOR, but the selected ones are the best

candidates. The WTR rating stays constant until 4 constraints are removed. This means that the constraint combinations identified up to 3 constraints (CP6, CP14, and CP10) that do not actively resist the most weakly constrained motion.

An important observation in this case study is that the maximum possible gain in TOR keeps increasing until removal of 4 constraints at a time (19% increase) and decreases afterwards. This means that removing 5 constraints from the assembly does not yield a better result compared to removing 4 constraints. In other words, a pattern of diminishing return occurs in the context of optimizing the assembly by reducing redundancy.

Another important observation is the final constraint configuration after 8 constraints are removed. At this point, the assembly is composed of 7 constraints. However, the constraint configuration here is different compared to the baseline model at the beginning of this case study. The reason is that in the constraint reduction scheme, constraints are removed from 15 to 7 in an optimal manner to maximize TOR increase. As a result, it is very likely that the final configuration is different and better than the baseline configuration. Table 11.6 shows the comparison between the 7-constraint baseline configuration and the 7-constraint improved configuration.

| | Baseline 7cp cube | Improved 7cp cube | % Difference |
|---|---|---|---|
| **WTR** | 0.200 | 0.340 | 41% |
| **MRR** | 1.000 | 1.000 | 0% |
| **MTR** | 0.486 | 0.572 | 15% |
| **TOR** | 0.486 | 0.572 | 15% |

**Table 11.6 Comparison between baseline and improved 7 constraint cube**

The constraint reduction scheme described in this section can be used as a design tool to optimize constraints by way of adding all possible constraint candidates and reducing until the desired number of constraints is reached. In this case, the procedure was:

1. The baseline model was composed of randomly selected 7 constraints to start with, assuming that 7 is the goal number of constraints.
2. All possible candidate constraints are added to the constraint configuration (in this case, up to 15 constraints).
3. Constraints are reduced optimally until the number of constraints is back to 7 (the goal number of constraint).

## 11.3 Simple rectilinear geometry – planar battery cover

These studies serve the purpose of verifying the agreement between the analysis and design tool and the design principles. Therefore, the actual amount of percentage increase or decrease in the overall ratings is of less interest.

### 11.3.1 Design principle test case study – leverage

The purpose of this case study is to verify that the design tool demonstrates the commonly known design principle of leverage. The goal of the optimization is to maximize the WTR rating. In order to simulate this, the optimization variables are the locations of constraints CP1 and CP3. The optimization variables and search space are specified in Table 11.7 and Figure 11.7.

| | Constraint variables | Line search center point | Line search direction | Move limits |
|---|---|---|---|---|
| **Variable group X1** | CP1 | $[1 \quad 2 \quad 0]$ | $[1 \quad 0 \quad 0]$ | $-1 \leq x_1 \leq 1$ |
| **Variable group X2** | CP3 | $[1 \quad 0 \quad 0]$ | $[1 \quad 0 \quad 0]$ | $-1 \leq x_2 \leq 1$ |

**Table 11.7 Optimization variables and search space for leverage case study**

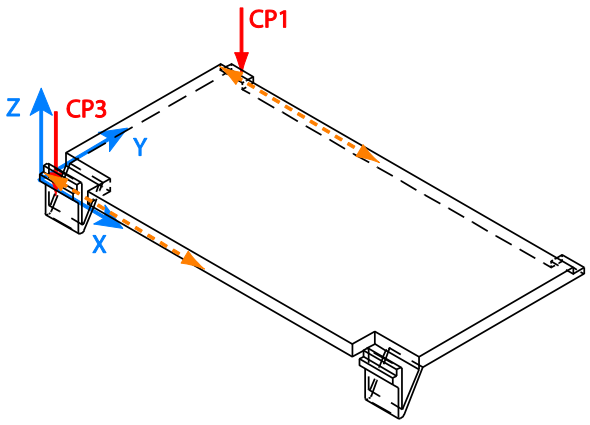


**Figure 11.7 Optimization variables and search space for leverage case study**

The response surface plot in Figure 11.8 shows that the constraints CP1 and CP3 reach optimal locations with respect to the WTR rating at the edge of the part. This confirms the design principle of leverage because constraints are more effective in resisting moments as they move to the edges of the part because of the increased moment arm for the reaction torque. The MTR plot also shows that CP1 and CP3 are most effective in resisting overall motion when they are located symmetrically with respect to the part. This principle of symmetry is tested in the case study described in the next section. The design therefore is already optimal by locating the snap-fit and lug at the edges of the part.

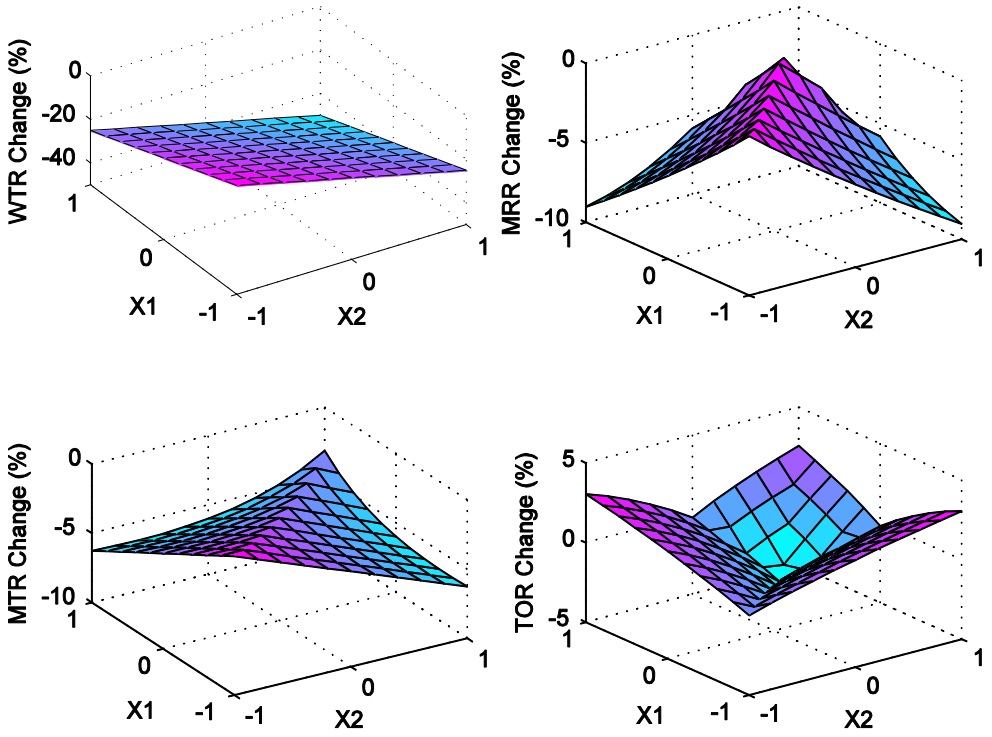


**Figure 11.8 Response surface plot for leverage design principle case study**

The MRR plot shows that redundancy is maximal at positions where CP1 and CP3 are parallel and symmetrical with respect to the part's line of symmetry. When CP1 and CP3 are located symmetrically, the pivot constraint combination that contains both CP1 and CP3 becomes a linearly dependent set of rank less than 5. This indirectly increases the redundancy of the constraint configuration. When CP1 and CP3 are perturbed from their symmetrical positions, the redundancy decreases. This is called the linear dependency bifurcation shift and will be discussed as a limitation of the response surface plots in Chapter 12. Because the MRR change is due to the linear dependency bifurcation point, the MRR does not accurately measure the true redundancy of the

assembly. The TOR plot increase at the edges of the move limits is mainly influenced by the reduction of redundancy. Therefore, the MRR and TOR plots are only useful when constraints are added or reduced. They are not of much interest in the context of constraint modification redesign because the number of constraints remains the same. From this point forward, comments on the MRR and TOR plot will be minimal unless constraint reduction or addition is involved.

### 11.3.2 Design principle test case study – symmetry

The purpose of this case study is to verify that the design tool demonstrates the commonly known design principle of symmetry. The goal of the optimization is to maximize the WTR rating. In order to simulate this, the baseline model is modified slightly. Instead of having two point constraints at the longer edge of the part (CP1, CP2, CP3, and CP4), one point constraint is placed on each edge (Figure 11.9, Table 11.8).

| | $P_x$ | $P_y$ | $P_z$ | $N_x$ | $N_y$ | $N_z$ |
|---|---|---|---|---|---|---|
| **CP1** | 2 | 2 | 0 | 0 | 0 | -1 |
| **CP2** | 2 | 0 | 0 | 0 | 0 | -1 |
| **CP3** | 0 | 1 | 0 | 0 | 0 | -1 |
| **CP4** | 4 | 1 | 0 | 0 | 0 | -1 |

**Table 11.8 Battery cover symmetry case study point constraint**

The locations of these constraints are the optimization variables. The constraints CP1 and CP2 are linked and move together along the top and bottom lines in the illustration, and constraints CP3 and CP4 are linked and move together along the side

lines in the illustration. The optimization variables and search space are specified in Table 11.9 and Figure 11.9.

| | Constraint variables | Line search center point | Line search direction | Move limits |
|---|---|---|---|---|
| **Variable group X1** | CP1, CP2 | $[2 \quad 2 \quad 0]$ | $[1 \quad 0 \quad 0]$ | $-1 \leq x_1 \leq 1$ |
| **Variable group X2** | CP3, CP4 | $[0 \quad 1 \quad 0]$ | $[0 \quad 1 \quad 0]$ | $-1 \leq x_2 \leq 1$ |

**Table 11.9 Optimization variables and search space for symmetry case study**

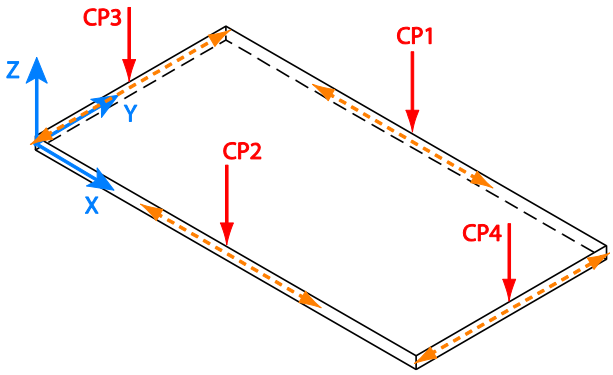


**Figure 11.9 Optimization variables and search space for symmetry case study**

The response surface plots (Figure 11.10) show that the constraints reach their optimal locations at the middle of the part where symmetry occurs both horizontally and vertically. This is applicable in optimizing the WTR as well as the MTR rating.

The following is an explanation for the WTR and MTR rating decrease as the constraints move away from their symmetrical locations. In this case, the screw axes of the reciprocal motions pass through the locations of some of the pivot constraints. Therefore, whenever one of the modified constraints (CP1, CP2, CP3, and CP4) is a

member of the pivot constraint combination, the reciprocal motion screw axis changes. A closer observation shows that the reason for the decrease in the WTR and MTR ratings is a consequence of the change in motion. This reveals that there are two different ways a rating can change (positively or negatively). One way is due to changing the locations or orientations of the constraints that actively resist a set of unchanged motions. The other way is due to changing the location or orientation of at least one of the constraints that belongs to the pivot constraints set, which then changes the reciprocal motion to be resisted by a set of unchanged constraints. In this case, the decrease is due to the latter.

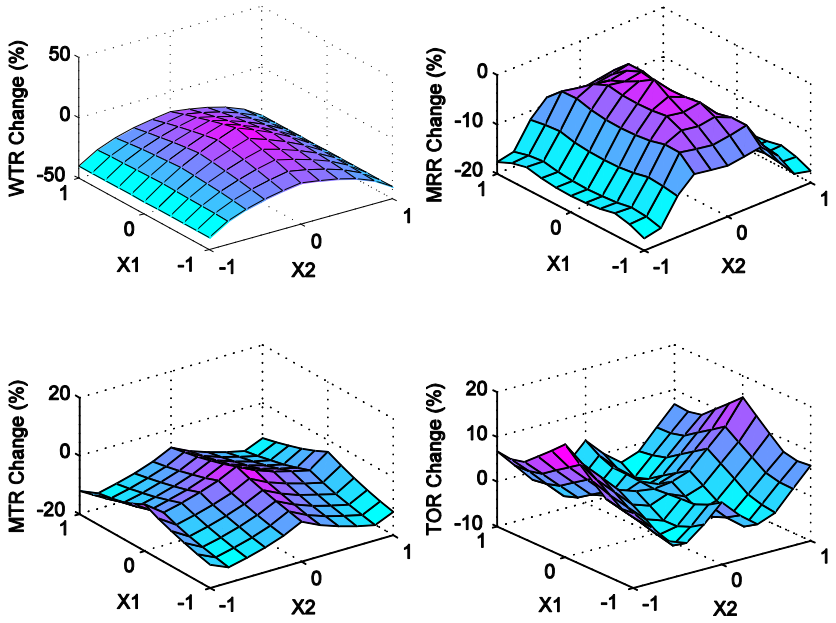


**Figure 11.10 Response surface plot for symmetry design principle case study**

Similar to the leverage case study in the previous section, the redundancy (MRR) is maximal where constraints are symmetrically located due to the fact that when

constraints are not symmetrical, they are less likely to be linearly dependent to the motions. This effect can be ignored in practical design applications. This is one of the limitations of this work and will be discussed in Chapter 12.

### 11.3.3 Study type: Design principle test – optimal line-of-action

The purpose of this case study is to confirm the design principle of line-of-action. The goal is to maximize the WTR rating. The optimization variables are the orientations of CP1, CP2, CP3, and CP4. The angular search space is the rotation about two different axes with a rotation angle limit of 45 degrees in both directions. The optimization variables and search space are specified in Table 11.10 and Figure 11.11.

| | Constraint variables | Orientation rotation axis | Rotation angle limits |
|---|---|---|---|
| **Variable group X1** | CP1, CP2, CP3, CP4 | $[1 \quad 0 \quad 0]$ | $-45° \leq \theta_1 \leq 45°$ |
| **Variable group X2** | CP1, CP2, CP3, CP4 | $[0 \quad 1 \quad 0]$ | $-45° \leq \theta_2 \leq 45°$ |

**Table 11.10 Optimization variables and search space for line-of-action case study**

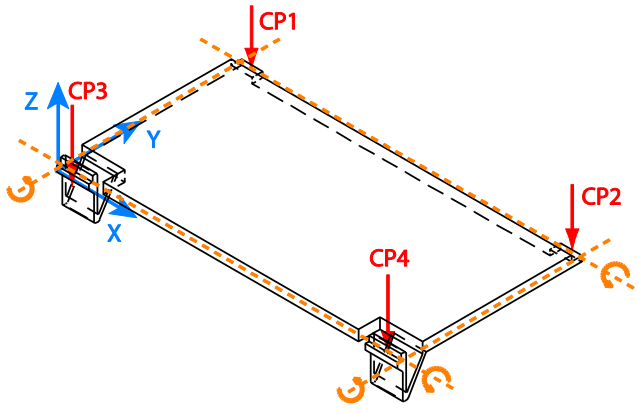


**Figure 11.11 Optimization variables and search space for line-of-action case study**

The response surface plot (Figure 11.12) for this case study shows that WTR reaches a maximum in the middle of the plot where the constraints are oriented perpendicular to the plane of the geometry (X1=0, X2=0). The WTR rating is the total resistance to this motion only. The orientation that provides optimal resistance with the least reaction force is the perpendicular orientation. This confirms the design principle of line-of-action.

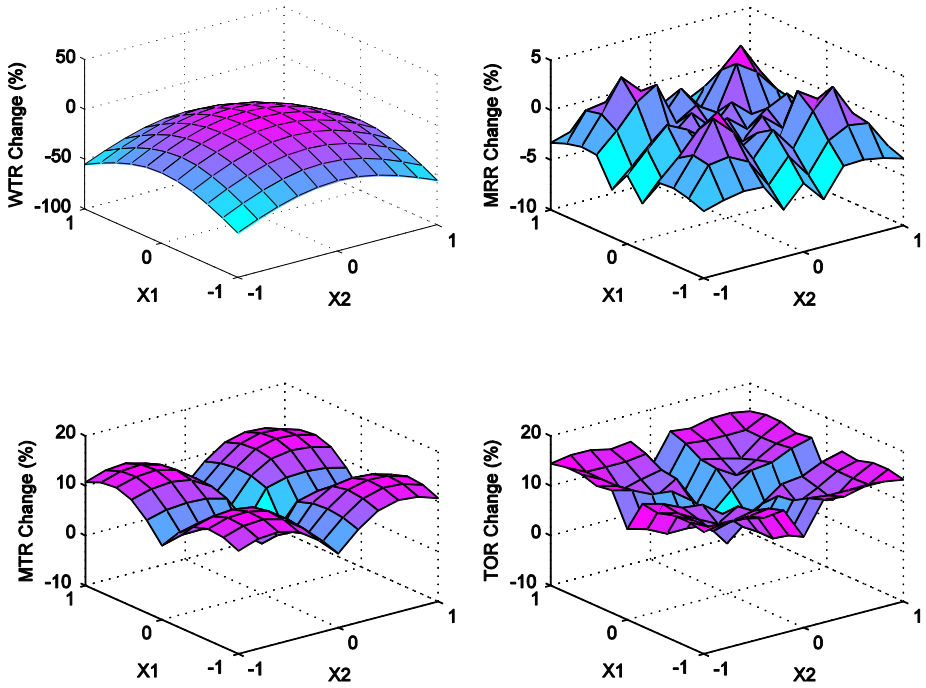


**Figure 11.12 Response surface plot for line-of-action design principle case study**

The MTR plot show that its maximum value occurs at a different angle. The reason for this is that the motion set changes significantly. A slight perturbation in the angular direction usually causes new motions that were not considered previously because the pivot constraint set was linearly dependent. The slight perturbation causes the constraint to be linearly independent from the set, although it is very close to being

linearly dependent. The new motions that are generated due to the new linearly independent pivot constraint set are usually rated as strongly resisted. This skews the average total resistance rating (MTR) to be higher. Due to this limitation, it is recommended that the orientation optimization be used only to optimize the most weakly constrained motion (WTR) or when critical or common design loading directions are known. The MRR plot shows many discontinuities due to the bifurcation shifts in linear dependency among constraints. This limitation will be discussed further in Chapter 12.

## 11.4 Axisymmetric geometry - end cap assembly

### 11.4.1 Design optimization case study – constraint addition

The purpose of this case study is to optimize the end cap assembly by adding constraints. The focus of this case study is to observe the extent to which adding constraints benefits the assembly and to identify the point of diminishing returns. In this case, the goal is to optimize the increase of the WTR and MTR ratings compared to the number of constraints being added. The constraint features being added are snap-fits around the lip of the end cap. The constraints are added as a set because each snap-fit is modeled as three unilateral point constraints. Figure 11.13 illustrates the radially symmetrical position of the snap-fits.

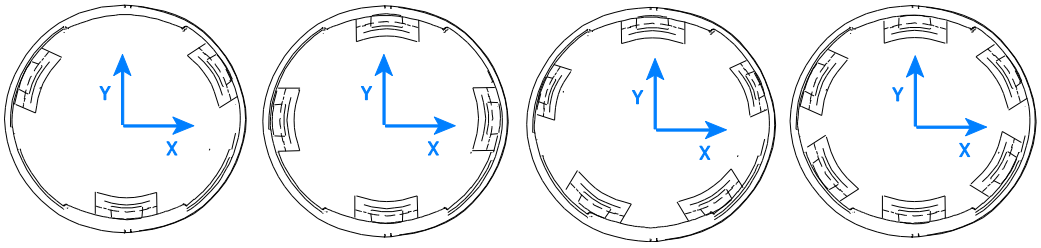


**Figure 11.13 End cap snap-fit addition configuration**

The plot in Figure 11.14 shows that adding more snap-fit features beyond 4 snap-fits does not yield any significant gain in the WTR rating. In addition, adding more snap-fit features beyond 5 does not yield any significant gain in any rating. As snap-fits are added, the MRR increases at the same rate as the MTR; therefore, the TOR remains approximately constant. This study is useful in determining the point at which adding more constraints, in this case more snap-fit features, yields diminishing returns in assembly rating.

The design recommendation based on these results is to increase the number of snap-fits up to 3 or 4. There is significant gain in the WTR for increasing from 2 to 3 snap-fits (68%) and from 3 to 4 snap-fits (32% additional). The trade-off ratio decreases, but the redundancy level at this point might be acceptable.

| No of snap-fits | WTR | MRR | MTR | TOR |
|---|---|---|---|---|
| 2 | 1.000 | 1.277 | 1.811 | 1.418 |
| 3 | 1.680 | 1.955 | 2.328 | 1.191 |
| 4 | 2.000 | 2.367 | 2.603 | 1.099 |
| 5 | 1.921 | 2.580 | 3.513 | 1.362 |
| 6 | 2.000 | 2.935 | 3.544 | 1.208 |

**Table 11.11 Rating change as the number of snap-fits is increased**

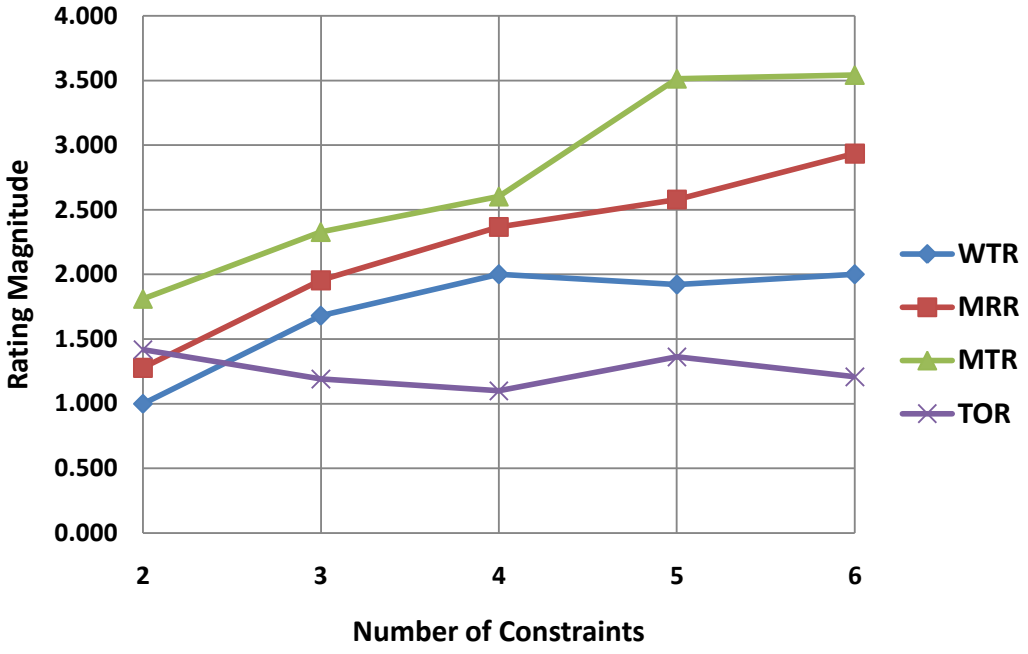


**Figure 11.14 Rating change as the number of snap-fits is increased**

### 11.4.2 Design optimization case study – snap-fit location

The purpose of this case study is to optimize the location of two of the snap-fits (CP1 through CP6) along the end cap lip curved line. The goal is to maximize the WTR rating. The optimization variables are the locations of two of the snap-fit features. The point constraints that are associated with a single feature are grouped and move together as the feature is modified. There are 3 point constraints that are associated with each snap-fit feature. Each snap-fit feature, however, is moved independently. Therefore, this is a 2-dimensional optimization search. The first group of variables (X1) consists of CP1, CP2, and CP3 and is associated with the first snap-fit feature. The second group of

variables (X2) consists of CP4, CP5, and CP6 and is associated with the second snap-fit feature.

The search space is a circular curve. The location of each snap-fit is varied along this curve. The circular search space is defined by an axis about which the snap-fit location is rotated. Table 11.12 specifies the optimization variables, the rotation axis location and orientation, and the rotation angle limits. Figure 11.15 illustrates the search space and move limits.

| | Constraint variables | Curved line search center of rotation | Curved line search rotation axis | Rotation angle limits |
|---|---|---|---|---|
| **Variable group X1** | CP1, CP2, CP3 | $[0 \quad 0 \quad 0]$ | $[0 \quad 0 \quad 1]$ | $-45° \leq \theta_1 \leq 45°$ |
| **Variable group X2** | CP4, CP5, CP6 | $[0 \quad 0 \quad 0]$ | $[0 \quad 0 \quad 1]$ | $-45° \leq \theta_1 \leq 45°$ |

**Table 11.12 Optimization variables and search space for snap-fit location**

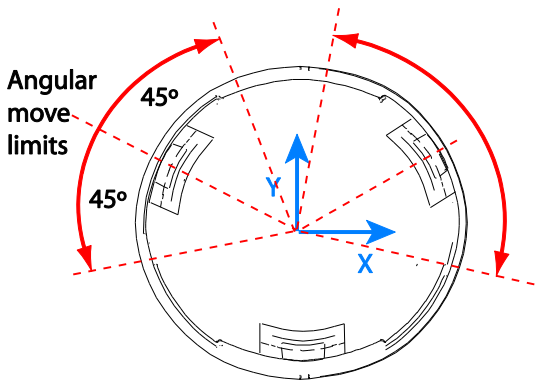


**Figure 11.15 Optimization variables and search space for snap-fit location**

The response surface plot is shown in Figure 11.16. It can be observed that WTR is maximal when the constraints are located in a radially symmetric pattern. The MTR

plot shows that rotating the snap-fit location up to approximately ±30 degrees does not immediately result in significant decrease in rating. Further rotation will decrease the MTR rating. The snap-fit is most effective when located at the radial symmetric position. This indirectly confirms the symmetry design principle discussed in the previous case study.

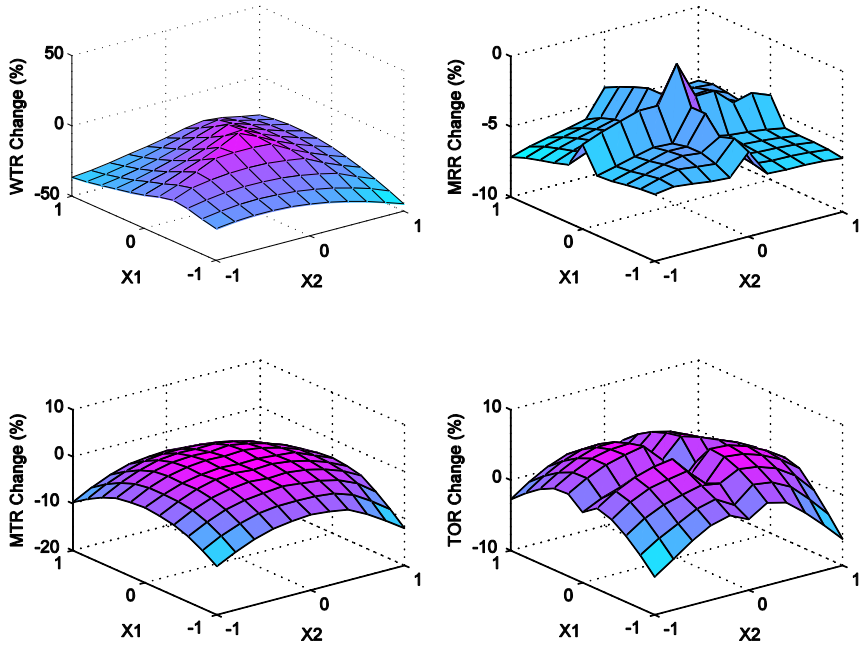


**Figure 11.16 Response surface cplot for end cap snap-fit location optimization**

It is also helpful to explore the areas in the WTR plot where the rating decreases significantly. The WTR rating decreases the most (up to more than 30%) as both snap-fits move closer to the bottom snap-fit and to each other. This causes all three snap-fits to be located in one half of the circular plane of the assembly. This constraint configuration and the most weakly constrained motion screw axis (zero-pitch) are illustrated in Figure 11.17. There is another weakly constrained motion screw axis that is symmetrical (in the

y-axis) to the one shown in the figure. The screw axis of the motion passes through two of the snap-fits' center locations and is resisted weakly by the third snap-fit.

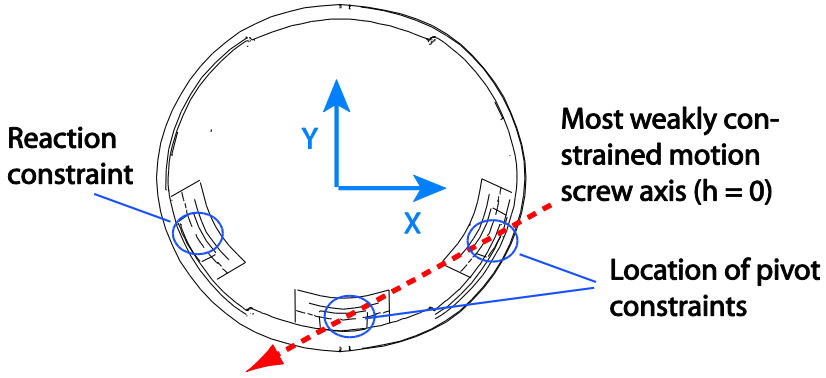


**Figure 11.17 Worst constraint configuration and its associated WTR motion**

### 11.5 Freeform/non-planar geometry - printer housing assembly

The following subsections explore the various search spaces available to the designer. In all these case studies, the manufacturability and cost to manufacture are ignored for design study purposes. Also, for visualization and design study purposes, the optimization for each design space in the following sections is limited to a two-dimensional search. Due to this limitation, each case study can only be done for a limited number of design variables. These localized design spaces are individually searched in a sequence of case studies, and at the end, the design spaces where possible improvements are identified are merged and searched simultaneously. An improved design recommendation for the printer housing based on the results is synthesized.

For all case studies under this section, the objective is to maximize the WTR rating. When there is no change in the WTR rating, maximizing the MTR rating becomes the secondary objective.

### 11.5.1 Design optimization – threaded fastener orientation search

The design space for the threaded fastener orientation is searched by allowing the orientation of all four fasteners to move in two angles (rotation around the x-axis and y-axis). The search space is defined as the rotation axes and the angular move limits. The optimization variables are shown in Figure 11.18 and listed in Table 11.13.

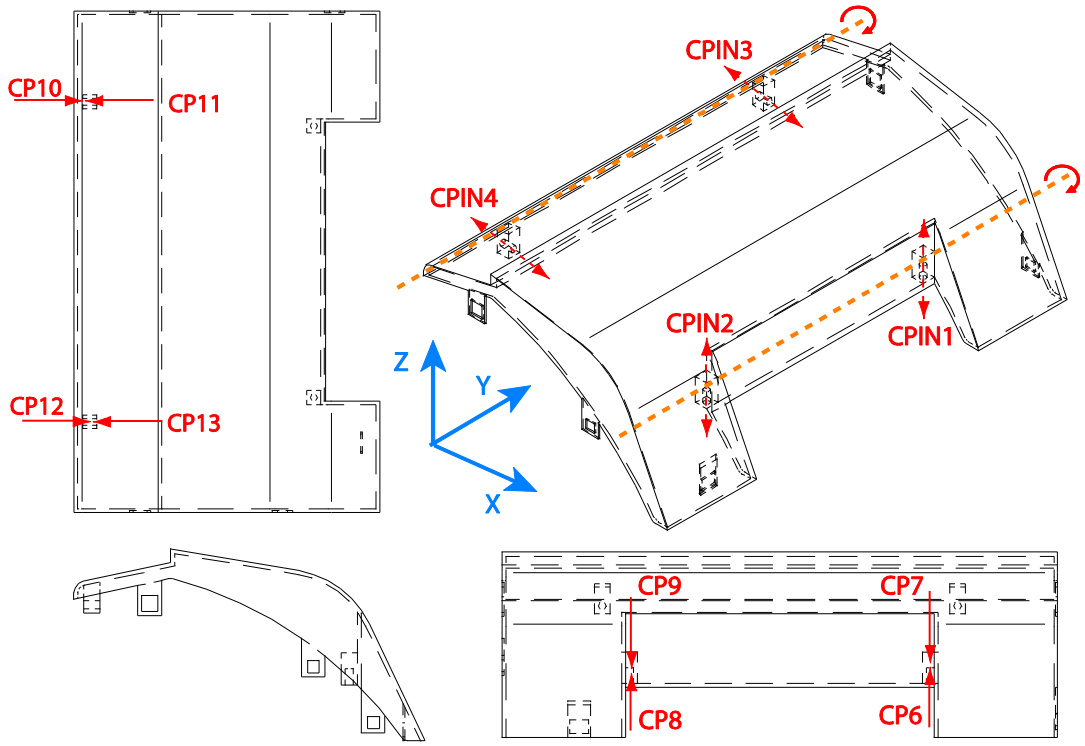


**Figure 11.18 Optimization variables and search space for fastener orientation**

There are two groups of variables. The first group of variables (X1) involves two fasteners near the bottom of the housing. The constraints that belong to this group are

CPIN1, CPIN2, CP6, CP7, CP8, and CP9. The second group (X2) consists of CPIN3, CPIN4, CP10, CP11, CP12, and CP13.

| | Variables | Orientation rotation axis | Rotation angle limits |
|---|---|---|---|
| **Variable group X1** | CPIN1, CPIN2, CP6, CP7, CP8, CP9 | $[0 \quad 1 \quad 0]$ | $-90° \leq \theta_1 \leq 90°$ |
| **Variable group X2** | CPIN3, CPIN4, CP10, CP11, CP12, CP13 | $[0 \quad 1 \quad 0]$ | $-90° \leq \theta_2 \leq 90°$ |

**Table 11.13 Optimization variables and search space for fastener orientation**

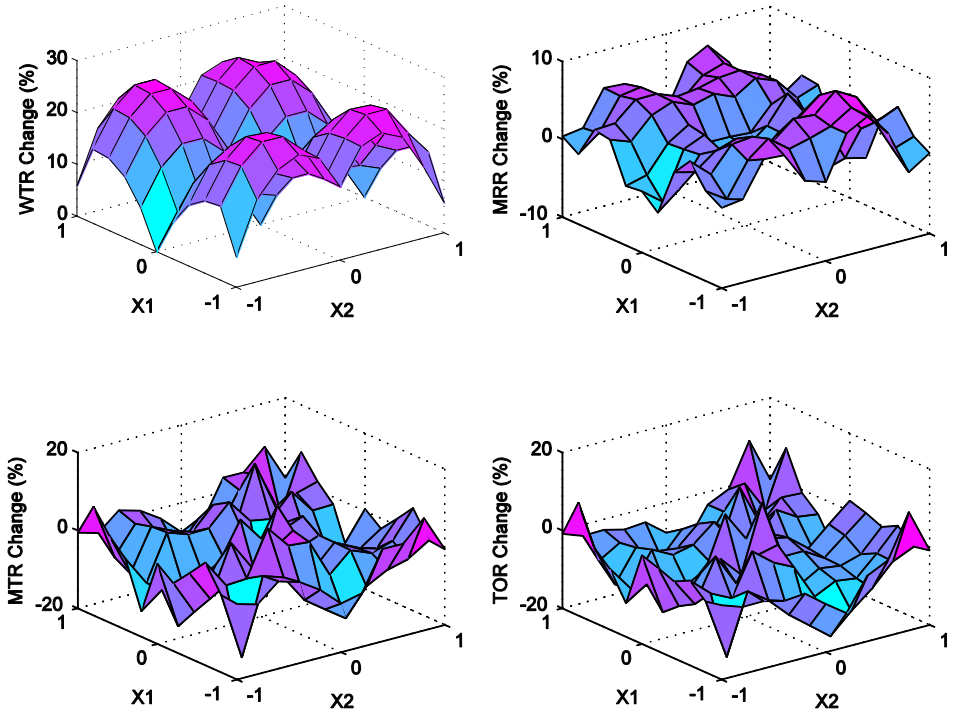


**Figure 11.19 Response surface plot for fastener orientation optimization**

The response surface plot is shown in Figure 11.19. In Section 11.1.2, it was explained that orientation searches yield more consistent results in the WTR rating; therefore, in this case, only the WTR plot is being evaluated. The WTR plot shows that

the WTR rating can be increased up to 24.6%. The WTR rating reaches a maximum value for the orientation combinations shown in Table 11.14 (all rotation is about the positive y-axis).

| | X1 Rotation about positive y-axis (degrees) | X2 Rotation about positive y-axis (degrees) | WTR change (%) |
|---|---|---|---|
| Optimum design 1 | 72 | -36 to -53 | 24.6% |
| Optimum design 2 | 72 | 36 to 53 | 24.6% |
| Optimum design 3 | -72 | -36 to -53 | 24.6% |
| Optimum design 4 | -72 | 36 to 53 | 24.6% |

**Table 11.14 Optimum design for fastener orientation search space**

This increase is due to the fact that the pivot constraint set for the WTR motion contains at least one of the modified constraints. As this constraint variable is modified, so is the motion reciprocal to the pivot constraints. The resulting motion is resisted more effectively and hence the WTR rating is improved.

As a side note, the MRR plot shows relatively random changes because of the of the linear dependency bifurcation shift. This is the one of the reasons MRR rating metric is irrelevant in orientation search spaces.

### 11.5.2 Design optimization – threaded fastener location

The design space for the threaded fastener location is searched by allowing the location of all four fasteners to move along two lines. The threaded fasteners at the locations of CPIN1 and CPIN3 are linked and move together. The same case applies for fasteners at the locations of CPIN2 and CPIN4. This is done to reduce the dimension of

the optimization search. The optimization variables and search space are specified in Table 11.15 and Figure 11.20.

| | Variables | Line search center point | Line search direction | Move limits |
|---|---|---|---|---|
| **Variable group X1** | CPIN1, CPIN3, CP6, CP7, CP10, CP11 | $[8.625 \quad 9 \quad 1.744]$ | $[0 \quad 1 \quad 0]$ | $-4.875 \leq x_1 \leq 4.875$ |
| **Variable group X2** | CPIN2, CPIN4, CP8, CP9, CP12, CP13 | $[8.625 \quad 9 \quad 1.744]$ | $[0 \quad 1 \quad 0]$ | $-4.875 \leq x_2 \leq 4.875$ |

**Table 11.15 Optimization variables and search space for fastener location**

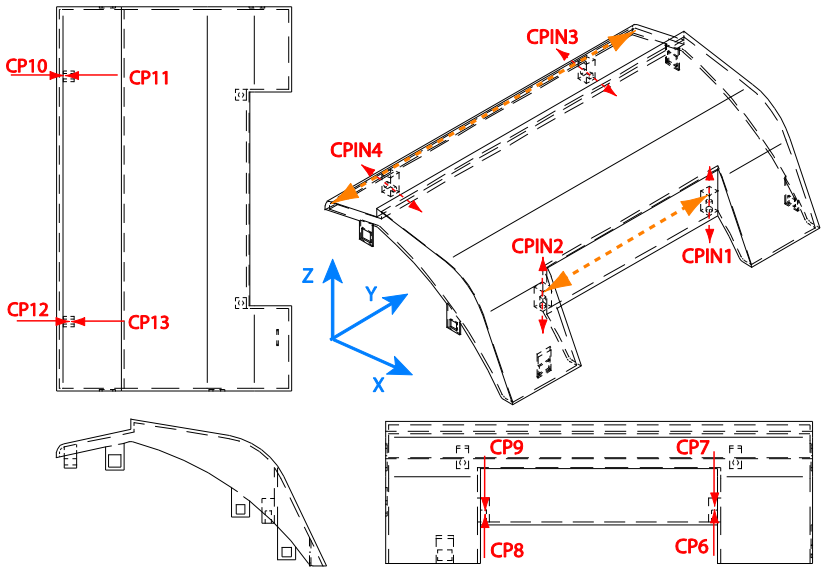


**Figure 11.20 Optimization variables and search space for fastener location**

The WTR plot in Figure 11.21 shows that the rating cannot be increased from the baseline model. The plot shows that the WTR rating is relatively constant for the cases where the two groups of fasteners are located symmetrically, namely they are the same

distance from the part symmetry line. The regions of the WTR plot where the rating decreases refer to locations where symmetry does not occur. The MTR plot also shows no improvement possible in this design space, but it is best to keep the fasteners at their original location. The discontinuity in the MTR plot is due to the fact that when the fastener locations coincide with one another, a certain motion set is eliminated due to linear dependency. The 'diagonal' in the MTR plot where the discontinuity occurs refers to the case where the four fasteners essentially become two fasteners because they overlap or almost overlap one another. The MRR plot shows that the redundancy is reduced at this overlapping location.

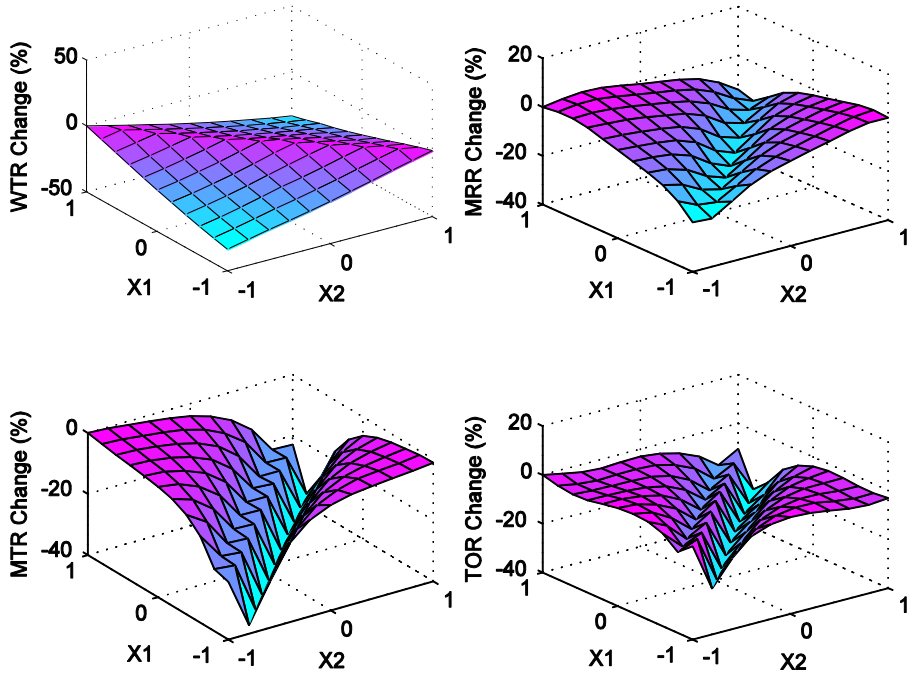


**Figure 11.21 Response surface plot for fastener location optimization**

Based on these results, there are two options. One is to keep the baseline design. The alternative is to reduce the number of fasteners from four to two and locate them along the line of symmetry. Table 11.16 shows that this reduction of fasteners yields a significant reduction in the redundancy ratio (MRR), which is desirable. This is done at the sacrifice of the WTR and MTR ratings. Overall, the alternate design is a better trade-off, shown by a higher TOR value. However, this is not an option when a decrease in WTR or MTR is not acceptable.

| | Baseline design with 4 fasteners | Alternate design with 2 fasteners | % Difference |
|---|---|---|---|
| **WTR** | 2.437 | 1.378 | -43.5% |
| **MRR** | 4.555 | 3.020 | -33.7% |
| **MTR** | 17.628 | 11.927 | -32.3% |
| **TOR** | 3.870 | 3.950 | 2.1% |

**Table 11.16 Comparison between assembly design with 4 vs. 2 fasteners**

### 11.5.3 Design optimization – snap-fit orientation

The design space for the snap-fit orientation is searched by allowing the orientations of four snap-fits (CP1, CP3, CP4, and CP5) to rotate around the y-axis. CP1 and CP5 are linked and rotated together. The same case applies for CP3 and CP5. This is done to reduce the dimension of the optimization search. The optimization variables and search space are specified in Table 11.17 and Figure 11.22.

| | Variables | Orientation rotation axis | Rotation angle limits |
|---|---|---|---|
| **Variable group X1** | CP1, CP5 | $[0 \quad 1 \quad 0]$ | $-60° \leq \theta_1 \leq 60°$ |
| **Variable group X2** | CP3, CP4 | $[0 \quad 1 \quad 0]$ | $-60° \leq \theta_1 \leq 60°$ |

**Table 11.17 Optimization variables and search space for snap-fit orientation**

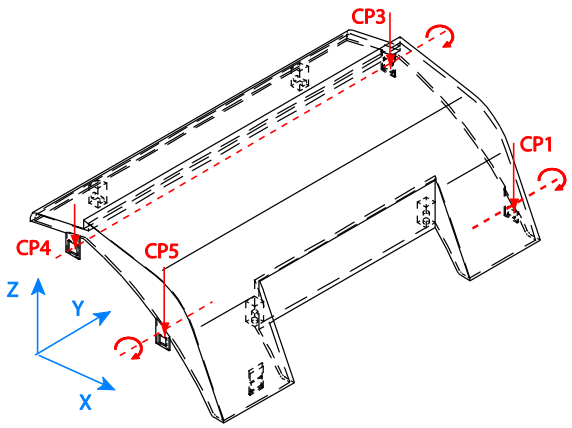


**Figure 11.22 Optimization variables and search space for snap-fit orientation**

The WTR plot (Figure 11.23) shows that an increase of 30.7% is achievable by re-orienting the snap-fits from the baseline model. There are two local maxima that can be identified (Table 11.18). In order to improve the rating, the two constraint variable orientations must be rotated in opposite directions. This is accomplished by rotating snap-fits CP1 and CP5 clockwise and snap-fits CP3 and CP4 counterclockwise about the y-axis. The design can also be improved by rotating snap-fits CP1 and CP5 counterclockwise and snap-fits CP3 and CP4 clockwise about the y-axis.

Although it was mentioned that manufacturing factors are not considered in this study, if this design were to be pursued, improved design #1 might be preferable because its normal direction is close to being perpendicular with the line constraints. This might reduce the mold complexity.

| | X1 Rotation (degrees) | X2 Rotation (degrees) | WTR change (%) |
|---|---|---|---|
| Optimum design 1 | 60 | -24 to -36 | 20.2% |
| Optimum design 2 | -12 to -60 | 60 | 30.5% |

**Table 11.18 Optimum design for snap-fit orientation search space**

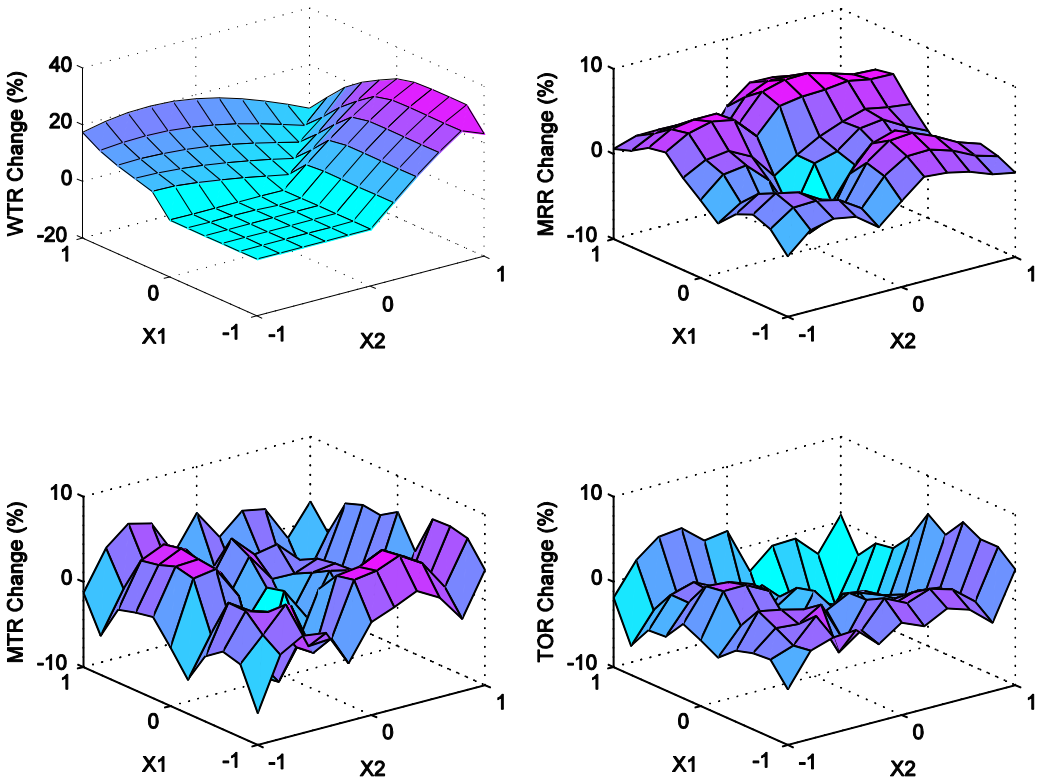


**Figure 11.23 Response surface plot for snap-fit orientation optimization**

### 11.5.4 Design optimization – snap-fit location

The design space for the snap-fit location is searched by allowing the locations of four snap-fits (CP1, CP3, CP4, and CP5) to move along the line constraints (CLIN1,

CLIN3, CLIN4, and CLIN2). The optimization variables and search space are specified in Table 11.19 and Figure 11.20.

| | Variables | Line search center point | Line search direction | Move limits |
|---|---|---|---|---|
| **Variable group X1** | CP1, CP5 | $[7.125 \quad 18 \quad 3.200]$ | $[-3.093 \quad 0 \quad 3.441]$ | $-4.5 \leq x_1 \leq 4.5$ |
| **Variable group X2** | CP3, CP4 | $[1.551 \quad 18 \quad 4.754]$ | $[2.000 \quad 0 \quad 0.431]$ | $-1.5 \leq x_2 \leq 1.5$ |

**Table 11.19 Optimization variables and search space for snap-fit location**

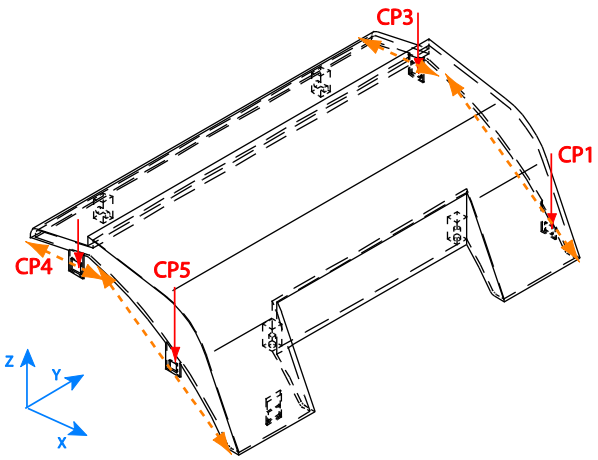


**Figure 11.24 Optimization variables and search space for snap-fit location**

The response surface plot (Figure 11.21) shows that the WTR rating does not change for any value of the optimization variables. A closer look at the rating matrix shows that the constraints being optimized are not active in resisting the most weakly constrained motion. MTR increases (4.5%) as the constraints CP1 and CP3 are moved higher along the line. The maximum for MTR occurs where CP1 is located between the

coordinates [5.320 18 5.208] and [5.922 18 4.539] along the line search. There is no effect on the MTR rating from moving CP4 and CP5.

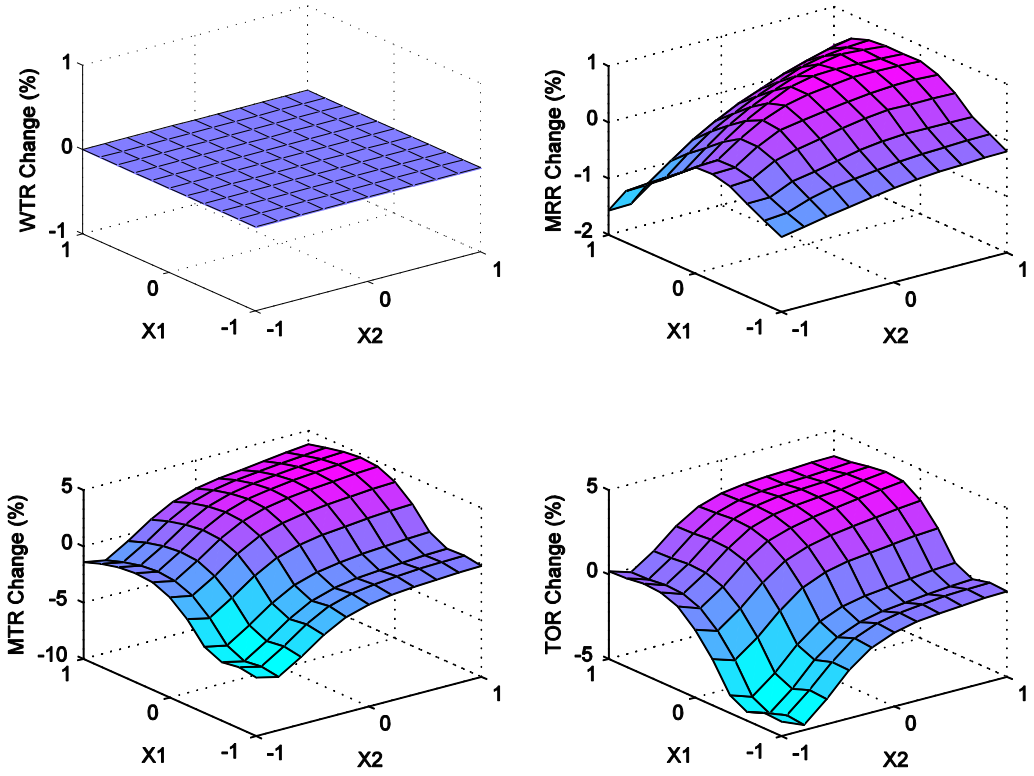


**Figure 11.25 Response surface plot for snap-fit location optimization**

### 11.5.5 Design optimization – parting line

The design space for the parting line is searched by allowing the orientations of line constraints CLIN1 and CLIN2 to be rotated about the y-axis. Rotating the orientation of the parting line, however, requires that CLIN3, CLIN4, CLIN5, and the two fasteners follow the parting line change by moving along the z-axis. Ideally, the two search spaces are linked, but this is not possible in the MATLAB script algorithm, so they are treated as

two independent design variables. The optimization variables and search space are specified in Table 11.20 and Figure 11.26.

| | Variables | Orientation rotation axis | | Rotation angle limits |
|---|---|---|---|---|
| **Variable group X1** | CLIN1, CLIN2 | $[0 \quad 1 \quad 0]$ | | $-60° \leq \theta_1 \leq 60°$ |
| | | **Line search center point** | **Line search direction** | **Move limits** |
| **Variable group X2** | CLIN5, CLIN3, CLIN4, CPIN3, CPIN4, CP3, CP4, CP10, CP11, CP12, CP13, | $[0 \quad 9 \quad 3]$ | $[0 \quad 0 \quad 1]$ | $-1 \leq x_1 \leq 1$ |

**Table 11.20 Optimization variables and search space for parting line**

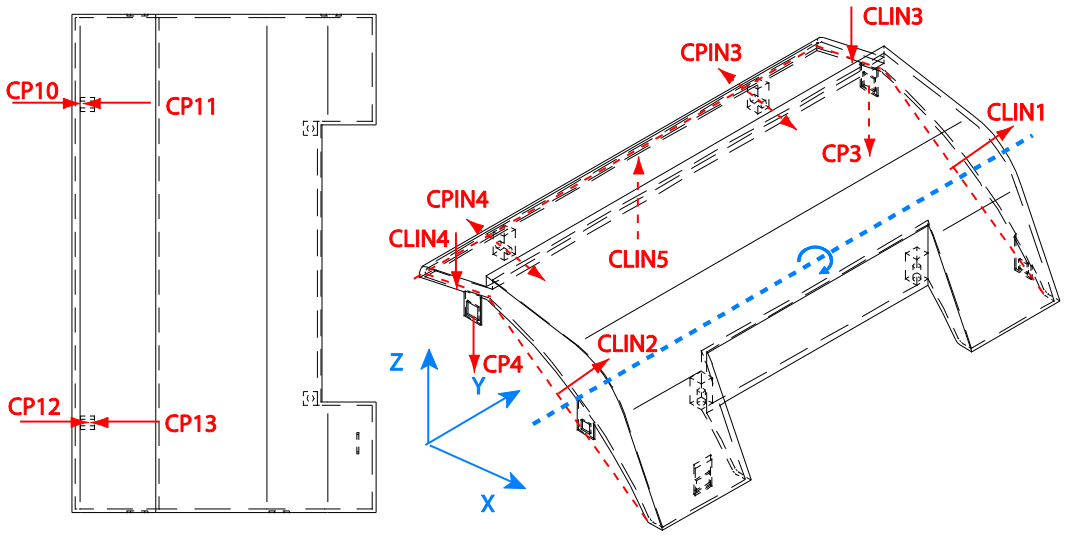


**Figure 11.26 Optimization variables and search space for parting line**

The response surface plot (Figure 11.27) shows that the WTR rating is only affected by the orientation of CLIN1 and CLIN2. There is no possible improvement from the baseline model by changing the variables in this case study, but the effect of rotating

the parting line orientation can be observed in the response surface plots. As CLIN1 and CLIN2 are rotated closer to the horizontal plane, the WTR rating decreases significantly. Rotating CLIN1 and CLIN2 in the opposite direction yields no gain in the WTR rating.

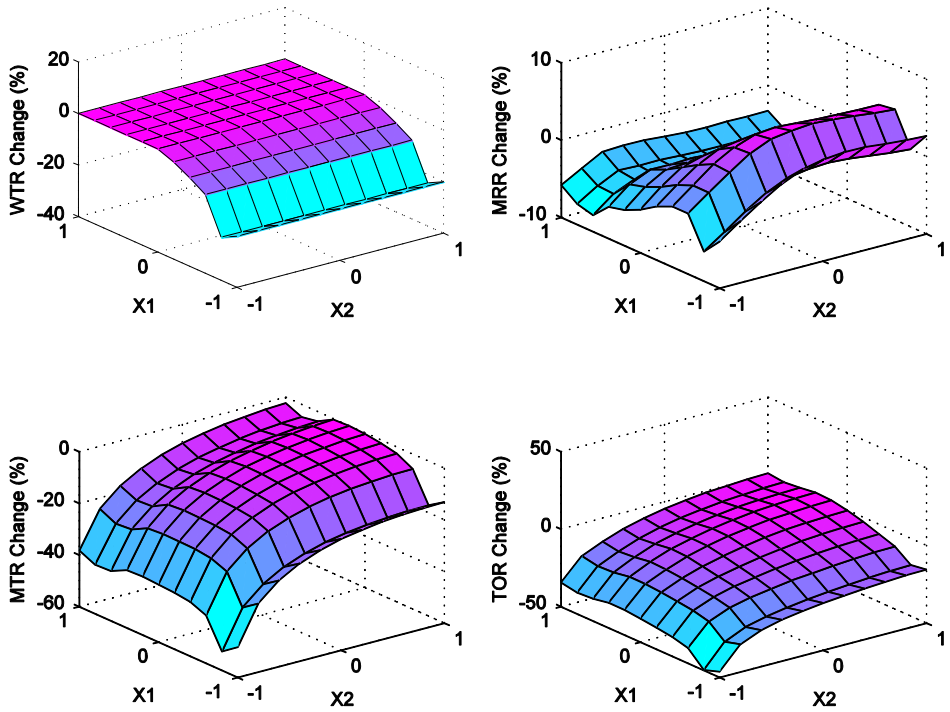


**Figure 11.27 Response surface plot for parting line optimization**

While moving the position of the second group of variables (CLIN3,CLIN4, CLIN5, and two fasteners on the top of the housing) in the z-direction does not affect the WTR rating, the effect on the MTR rating is significant. The MTR plot shows that not only does rotating the parting line toward the XY plane decrease the rating, but lowering the position of the second group of variables in the z-direction amplifies the rating decrease. There is a slight interaction between the two design search spaces.

These results show that the baseline design of the parting line already yields maximum WTR and MTR ratings. If the printer housing were designed with the

traditional planar parting line (X1= -1), the rating would be much lower than the baseline results (Table 11.21).

| | Baseline design with non-planar parting line | Alternate design with horizontal parting line | % Difference |
|---|---|---|---|
| **WTR** | 2.437 | 1.869 | -23.3% |
| **MRR** | 4.555 | 4.577 | 0.5% |
| **MTR** | 17.628 | 13.295 | -24.6% |
| **TOR** | 3.870 | 2.905 | -24.9% |

**Table 11.21 Comparison of non-planar parting line vs. planar parting line design**

### 11.5.6 Design optimization – line constraint length

There are two case studies done to search the line constraint length design space. The first study involves the lines CLIN5 and CLIN6 as the optimization variables. The second study involves the lines CLIN1, CLIN2, CLIN3, and CLIN4.

For the first line size search study, the optimization variables and search space are specified in Table 11.22 and Figure 11.28. The second line size search study optimization variables and search space are specified in Table 11.23 and Figure 11.29. In the second study, to maintain geometric compatibility, the length of CLIN1 must be inversely proportional to the length of CLIN3. In the same way, the length of CLIN2 must be inversely proportional to the length of CLIN4. However, this relationship cannot be programmed in the MATLAB script, and therefore they are treated as separate optimization variable groups.

| | Variables | Line length limits |
|---|---|---|
| **Variable group X1** | CLIN5 | $8.5 \leq L_1 \leq 14.5$ |
| **Variable group X2** | CLIN6 | $15 \leq L_2 \leq 21$ |

**Table 11.22 Optimization variables and search space for line size (CLIN5, CLIN6)**

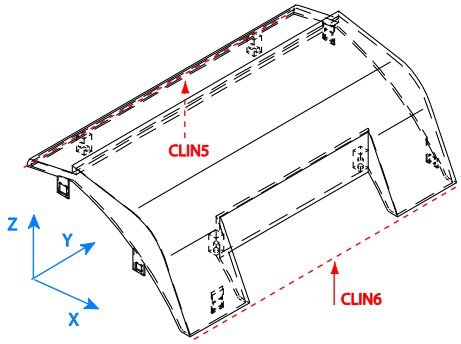


**Figure 11.28 Optimization variables and search space for line size (CLIN5, CLIN6)**

| | Variables | Line length limits |
|---|---|---|
| **Variable group X1** | CLIN1, CLIN2 | $7 \leq L_1 \leq 11$ |
| **Variable group X2** | CLIN3, CLIN4 | $1 \leq L_2 \leq 5$ |

**Table 11.23 Optimization variables and search space for line size (CLIN1-CLIN4)**

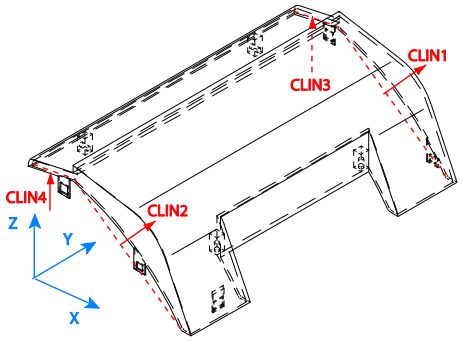


**Figure 11.29 Optimization variables and search space for line size (CLIN1-CLIN4)**

The response surface plots in Figure 11.30 and Figure 11.31 show that both the WTR and MTR ratings would be maximal when the lengths of the line constraints are the

longest. The reason is that a longer line has a greater moment arm length to resist moment loads. Since the line constraints in the baseline model are at maximum length, there is no further design improvement possible. There is no effect on the WTR rating because the optimization variables in this particular case are not active in resisting the WTR motion.

The design implication of this study is that a line constraint size is always optimal at its longest allowable length. The same case applies for the area of a planar constraint.

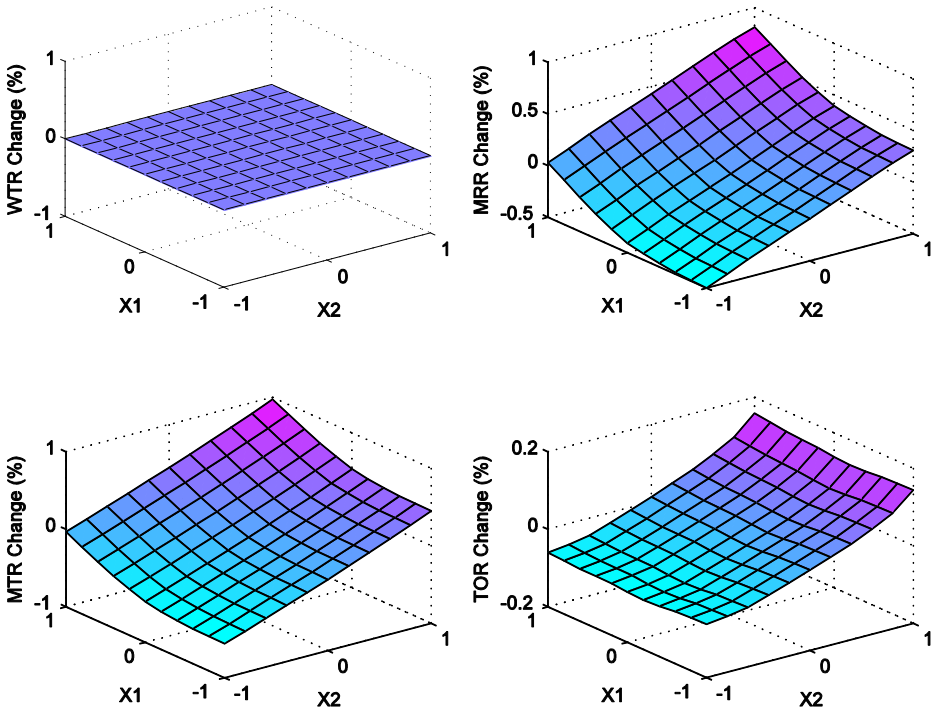


**Figure 11.30 Response surface plot for line size optimization (CLIN5, CLIN6)**

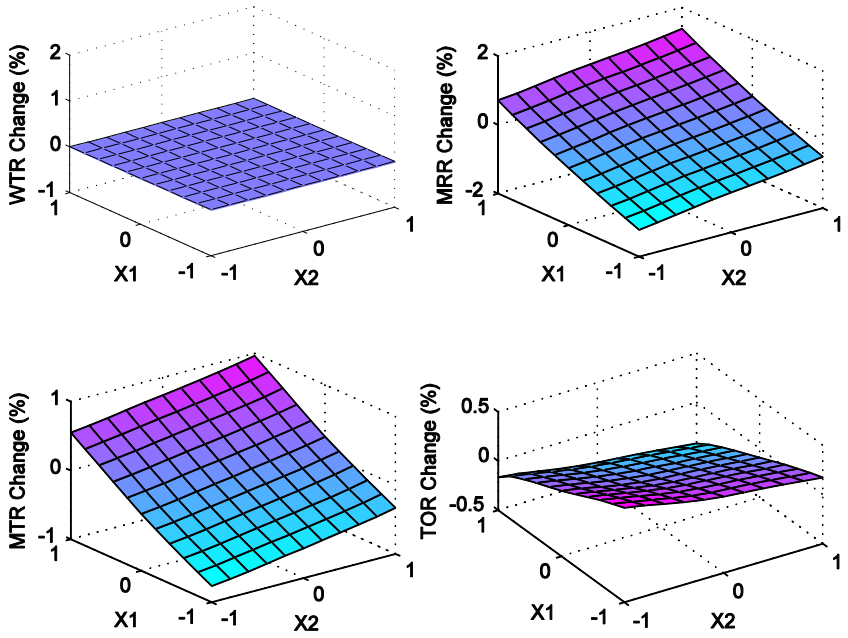


**Figure 11.31 Response surface plot for line size optimization (CLIN1-CLIN4)**

### 11.5.7 Synthesis of improved design

The design study conclusions on the printer housing are summarized in Table 11.24. Based on the design space exploration, a few design recommendations can be suggested. Table 11.25 summarizes the possible design improvements for the printer housing based on the results of the optimization studies done so far.

| Optimization Study | Optimization variables | Search type | Study conclusions |
|---|---|---|---|
| Fastener orientation search | CPIN1, CPIN2, CP6, CP7, CP8, CP9 | Orientation | 24.6% improvement in WTR is possible |
| | CPIN3, CPIN4, CP10, CP11, CP12, CP13 | Orientation | |
| Fastener location search | CPIN1, CPIN3, CP6, CP7, CP10, CP11 | Line search | No improvement possible, keep baseline design. 2 fastener design increases TOR by 12.8% |
| | CPIN2, CPIN4, CP8, CP9, CP12, CP13 | Line search | |
| Snap-fit orientation search | CP1, CP5 | Orientation | 30.7% improvement in WTR is possible |
| | CP3, CP4 | Orientation | |
| Snap-fit location search | CP1, CP5 | Line search | 4.5% improvement in MTR is possible |
| | CP3, CP4 | Line search | |
| Parting line search | CLIN1, CLIN2 | Line direction orientation | Non-rectilinear parting line is prefered, which is the baseline design. Traditional horizontal parting line decreases WTR by 23.3% and MTR by 24.6% |
| | CLIN5, CLIN3, CLIN4, CPIN3, CPIN4, CP3, CP4, CP10, CP11, CP12, CP13, | Line search | |
| Line length search | CLIN5 | Line size search | No improvement possible, keep line the longest possible without increasing overall part size. |
| | CLIN6 | Line size search | |
| | CLIN1, CLIN2 | Line size search | |
| | CLIN3, CLIN4 | Line size search | |

**Table 11.24 Summary of design study conclusions**

| | Case Study | Design Change |
|---|---|---|
| **Design revision A** | Fastener orientation search | Rotate (CPIN1, CPIN2, CP6, CP7, CP8, CP9) 72 degrees and rotate (CPIN3, CPIN4, CP10, CP11, CP12, CP13) -36 degrees about the y-axis |
| **Design revision B** | Snap-fit orientation search | Rotate CP1, CP5 -12 to -60 degrees and rotate CP3, CP4 60 degrees about the y-axis |
| **Design revision C** | Snap-fit location search | Move CP1 and CP5 to X=5.320, Z=5.208 |

**Table 11.25 Summary of design recommendation for each design revision**

The design improvements for each design space can be implemented one at a time. In this section, an attempt to merge these design changes and observe whether the assembly rating improvements accumulate is done. When design changes involving multiple variables are done simultaneously, there is a possibility of interaction between the factors being changed. In order to identify a simultaneous search optimum involving all factors that allow improvements in assembly rating, a higher dimensional search must be done. The current MATLAB script allows up to a five-dimensional search. Due to limitations in computational capability, the number of increments in this search is limited to 6. This slightly reduces the accuracy of the results. The variables identified for improving the assembly configuration are

- Orientation of two threaded fasteners (2D search)
- Orientation of four snap-fits (CP1, CP3, CP4, and CP5) (2D search)
- Location of two snap-fits (CP1 and CP3) (1D search)

A search of the specified design space for all five optimization variables was conducted. The objective is to maximize the WTR rating. The optimum point within the optimization constraints and the corresponding design change is shown in Table 11.26.

| | Normalized Units | Optimization variables | Search type | Design Change |
|---|---|---|---|---|
| **X1** | -1.0 or 1.0 | CPIN1, CPIN2, CP6, CP7, CP8, CP9 | Orientation | Rotate CPIN1, CPIN2, CP6, CP7, CP8, and CP9 90 or -90 degrees about the y-axis |
| **X2** | -0.6 | CPIN3, CPIN4, CP10, CP11, CP12, CP13 | Orientation | Rotate CPIN3, CPIN4, CP10, CP11, CP12, and CP13 -54 degrees about the y-axis |
| **X3** | 0.6 | CP1, CP5 | Orientation | Rotate CP1 and CP5 54 degrees about the y-axis |
| **X4** | -0.6 | CP3, CP4 | Orientation | Rotate CP3 and CP4 -54 degrees about the y-axis |
| **X5** | -0.6 | CP1, CP5 | Location | Move CP1 to [7.526 18 2.754] and CP5 to [7.526 0 2.754] |

**Table 11.26 Simultaneous search optimum in the design search space**

Based on this higher dimension optimum search, the design recommendations for only some variables are similar to those in Table 11.25. The recommended design change for variable group X1 and X2 is similar to the previous results when the design spaces were searched individually. This difference can be attributed to interactions among the design variables and/or to the reduction of the search resolution. The design recommendations for X3 and X4 are different. They are oriented in the opposite direction compared to the previous design recommendation. However, based on Figure 11.23, this new design recommendation still falls near to the local optimum in the response surface plot. The design recommendation for X5 is also different. For variable X5, the design

recommendation is to move CP1 and CP5 in the opposite direction. Recall that in the individual design space study (Section 11.5.4) the design recommendation is based on the MTR rating improvement, not the WTR rating. This might be the reason for the difference in design change recommendation.

For this particular case study, orientation modification is more effective in improving WTR and location modification is more effective in improving MTR. The difference between the individual optimization searches and the higher dimension optimization search shows that there are interactions among the design variables. Therefore, it is important to search the design space simultaneously when multiple design variables are involved.

Table 11.27 and Figure 11.32 summarize the design improvements across the possible design revisions. It is found that the optimum (design revision D) has the best WTR rating, but is not best in all ratings. Furthermore, the rating gains obtained by individual design changes do not always accumulate when all of them are implemented. In a real design context, more design changes lead to higher cost, except when done in the conceptual design stage. In this context, it is important to observe that the assembly rating improvement does not necessarily accumulate with each design change implementation.

| | WTR | | MRR | | MTR | | TOR | |
|---|---|---|---|---|---|---|---|---|
| | Rating | % Diff. | Rating | % Diff. | Rating | % Diff. | Rating | % Diff. |
| Baseline design | 2.437 | | 4.555 | | 17.628 | 0.0% | 3.870 | |
| Design revision A | 3.036 | 24.6% | 4.806 | 5.5% | 17.203 | -2.4% | 3.579 | -7.5% |
| Design revision B | 3.180 | 30.5% | 4.562 | 0.1% | 18.827 | 6.8% | 4.075 | 5.3% |
| Design revision C | 2.437 | 0.0% | 4.564 | 0.2% | 18.421 | 4.5% | 3.994 | 3.2% |
| Design revision D | 3.507 | 43.9% | 4.766 | 4.6% | 18.323 | 3.9% | 3.844 | -0.7% |

**Table 11.27 Summary of design alternative ratings**

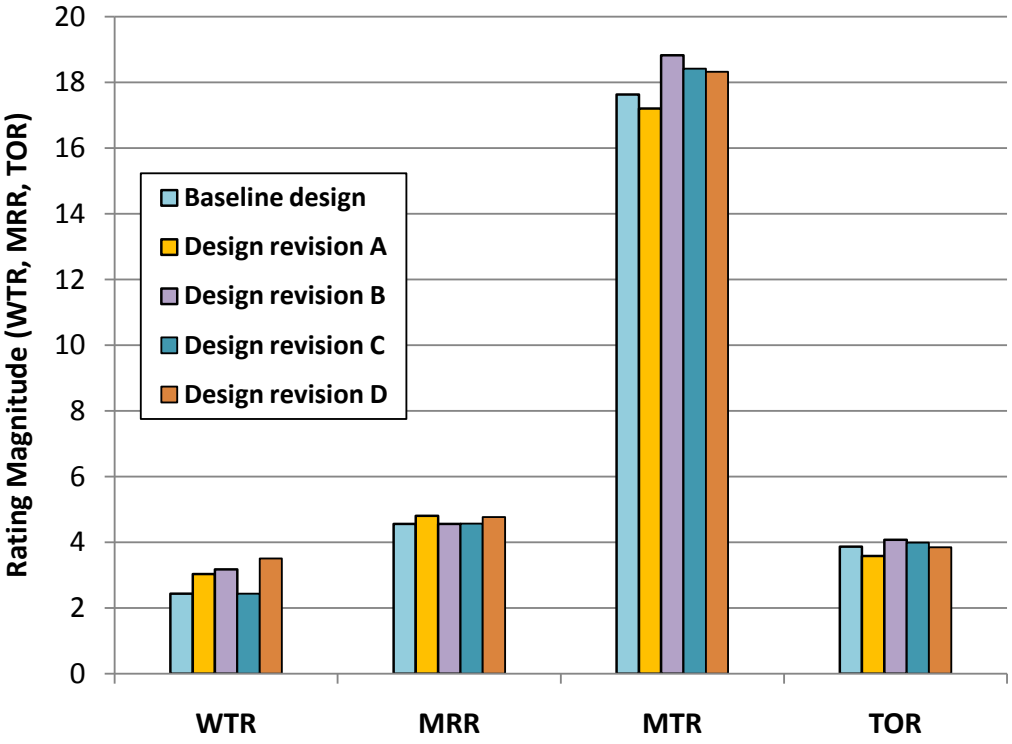


**Figure 11.32 Summary of design alternative ratings**

### 11.5.8 Design optimization - known loading direction

The purpose of this study is to optimize the constraint configuration for a specified loading condition. In this case, the specified motion is a pure rotation around the screw axis

$$\omega = [0 \quad 1 \quad 0], \rho = [2 \quad 0 \quad 4], h = 0$$

The optimization variables chosen for this study are the same as in the snap-fit location optimization case study. The optimization variable and search space are identical to Table 11.19 and Figure 11.24.

Note that for this response surface plot (Figure 11.33), the vertical axis is in absolute value, not a percent change. Since there is only one motion being evaluated, only the WTR plot is of interest. The response surface plot shows that the location of variable group X2 (CP3 and CP4) does not affect the WTR rating. The location of variable group X1 (CP1 and CP5) is better at X1=-1. This is contradictory to the results in Section 11.5.4. The recommended modification in the study where the design space is only comprised of the line search is to move the constraints CP1 and CP5 closer to CLIN3 and CLIN4. In this study, the recommended modification is to move CP1 and CP5 away from CLIN3 and CLIN4. Therefore, when a constraint configuration is optimized for a particular loading condition, the overall rating of the assembly might actually decrease from the baseline design.

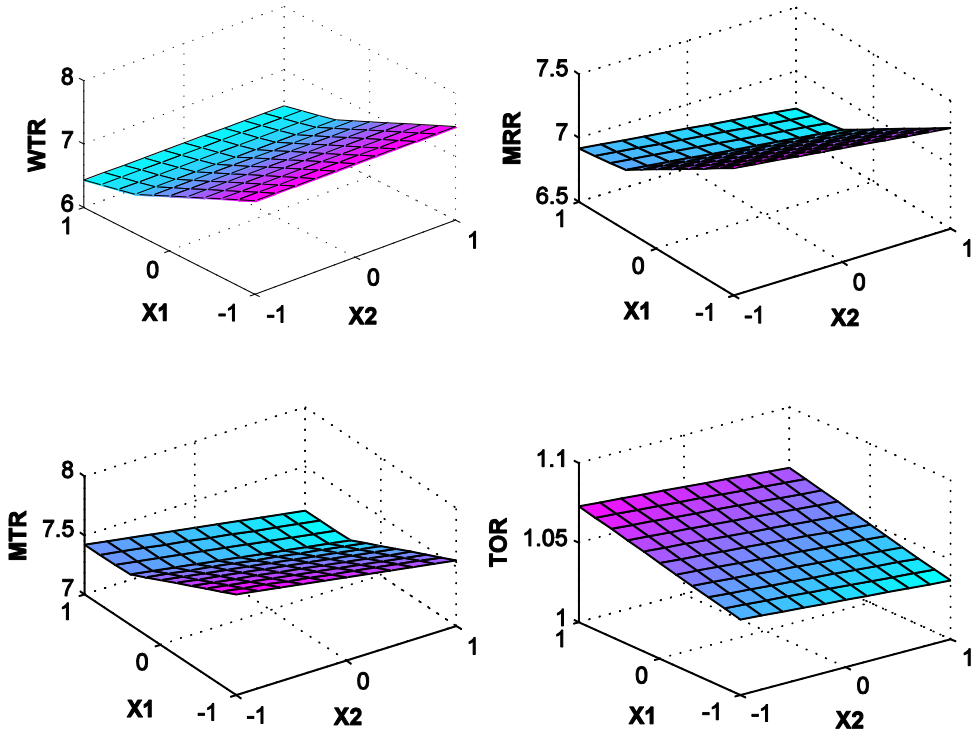


**Figure 11.33 Response surface plot for snap-fit location optimization (specified loading condition)**

### 11.5.9 Design optimization – constraint reduction

The purpose of this study is to apply the constraint reduction scheme to the printer housing case study. The goal in this study is to maximize the trade-off ratio (TOR). The constraint reduction scheme shows that the trade-off ratio can be increased significantly as more constraints are removed (Figure 11.34). The selected constraints to remove that yield the most TOR increase are shown in Table 11.28. Constraint index 15, 16, 17 occur frequently as the most appropriate constraints to remove in order to decrease redundancy with minimal impact on MTR. These constraint indexes refer to CPIN2, CPIN3, and

CPIN4. Unfortunately, the removal of the fasteners that are represented by these pin constraints also eliminates the point constraints associated with them.

| No of Constraints removed | Maximum Possible TOR increase (%) | WTR | MRR | MTR | TOR | Removed Constraints Index | | | | | | |
|---|---|---|---|---|---|---|---|---|---|---|---|---|
| 0 | 0.0% | 2.437 | 4.555 | 17.628 | 3.870 | | | | | | | |
| 1 | 3.9% | 2.437 | 4.354 | 17.500 | 4.019 | 1 | | | | | | |
| 2 | 6.1% | 2.437 | 4.237 | 17.399 | 4.106 | 6 | 7 | | | | | |
| 3 | 17.3% | 1.290 | 4.044 | 18.360 | 4.540 | 10 | 11 | 15 | | | | |
| 4 | 21.5% | 1.290 | 3.811 | 17.926 | 4.704 | 1 | 10 | 11 | 15 | | | |
| 5 | 27.4% | 1.000 | 2.909 | 14.344 | 4.931 | 8 | 9 | 14 | 16 | 17 | | |
| 6 | 38.7% | 1.000 | 2.639 | 14.167 | 5.368 | 1 | 6 | 7 | 15 | 16 | 17 | |
| 7 | 45.6% | 1.000 | 2.329 | 13.125 | 5.635 | 1 | 6 | 7 | 15 | 16 | 17 | 18 |

**Table 11.28 Effect of constraint reduction to assembly rating for printer housing**

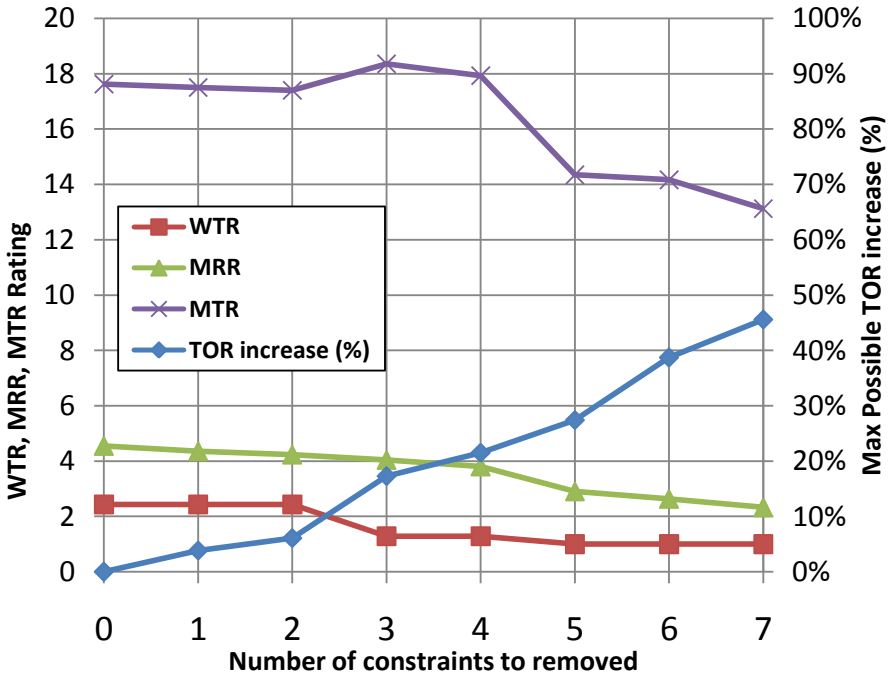


**Figure 11.34 Effect of constraint reduction to assembly rating for printer housing**

While removing more than 2 constraints yields even greater gain in the TOR, the WTR rating decreases significantly. Removing more than 2 constraints reduces the WTR rating from 2.437 to 1.290. This is about a 47% decrease. Note that the TOR is the ratio between MTR and MRR without regard to the WTR rating. Therefore, to minimize the impact on the WTR rating, the constraint removal should be limited to 2 constraints.

The result shows that CP6 and CP7 are the candidate constraints to be removed. The fastener that represents these pin constraints is also associated with CPIN1. In order to remove CP6 and CP7, CPIN 1 (one threaded fastener) must also be removed. An analysis of the design with the whole threaded fastener removed yields a decrease of 59% in the WTR rating. Therefore, the two-way constraints CP6 and CP7 must be removed without removing the pin constraint. This can be done by modifying or "downgrading" the assembly feature from a threaded fastener to a locating pin. This shows the advantages of integral attachment features compared to traditional bolted joints. In addition, integral attachment features provides more flexibility by allowing the removal of fewer DOF at a time during constraint reduction scheme. Table 11.29 shows the results for removing CP6 and CP7, labeled as alternate design 1.

Another alternative is to apply the same feature downgrading technique to the other threaded fasteners. Alternate design 2 is the case where the threaded fastener associated with CPIN2 is transformed into pin constraints and alternate design 3 is the case where all threaded fastener is transformed to pin constraints. Table 11.29 shows that the recommended design is alternate design 2 because there is very minimal decrease in WTR but much reduction in redundancy. This can also be observed in the TOR increase.

Alternate design 3 offers more reduction of redundancy, but at this point, the WTR rating decreases 35%.

| | Baseline design | Alternate design 1 (CP6, CP7 removed) | % Diff. | Alternate design 2 (CP6-CP9 removed) | % Diff. | Alternate design 3 (CP6-CP13 removed) | % Diff. |
|---|---|---|---|---|---|---|---|
| **WTR** | 2.437 | 2.4367 | 0.0% | 2.4367 | 0.0% | 1.578 | -35.2% |
| **MRR** | 4.555 | 4.2372 | -7.0% | 3.989 | -12.4% | 3.5283 | -22.5% |
| **MTR** | 17.628 | 17.3993 | -1.3% | 17.3467 | -1.6% | 14.8045 | -16.0% |
| **TOR** | 3.870 | 4.1063 | 6.1% | 4.3487 | 12.4% | 4.1959 | 8.4% |

**Table 11.29 Comparison of rating between baseline and alternate designs for constraint removal (printer housing)**

### 11.5.10 Sensitivity analysis

The sensitivity of each constraint's location and orientation is evaluated. In this case a position perturbation of 0.5 inch (about 2-3% of overall part length) and an orientation perturbation of 10° are applied. Table 11.30 summarizes the change in rating due to perturbation in each rating. It can be observed that the WTR rating is most sensitive when CPIN1 and CPIN2 are deactivated, CLIN1 and CLIN2 position perturbed, and CLIN3 and CLIN4 orientations perturbed. The toggle perturbation has a much more significant effect compared to a position or orientation perturbation because in toggle perturbation the constraint is removed instead of being perturbed. Constraints that show zero percent change when perturbed are either not actively resisting the WTR motion or their perturbations do not change the resistance quality of the respective constraints.

As a result of the sensitivity study, the constraints that are more critical to deliver the intended performance of the assembly are identified. In the tooling design, certain

decisions such as the location of gates and cooling lines in the mold influence the areas that are subject to more shrinkage than others and directions in which warpage occurs. The identification of critical constraints might influence these tooling design decisions or vice versa.

| | Toggle Perturbation WTR Change (%) | Position Perturbation worst WTR Change (%) | Orientation perturbation worst WTR Change (%) |
|---|---|---|---|
| **CP1** | 0.0% | 0.0% | 0.0% |
| **CP2** | 0.0% | 0.0% | -0.2% |
| **CP3** | 0.0% | 0.0% | -0.2% |
| **CP4** | 0.0% | 0.0% | -0.2% |
| **CP5** | 0.0% | 0.0% | 0.0% |
| **CP6** | 0.0% | 0.0% | 0.0% |
| **CP7** | 0.0% | 0.0% | 0.0% |
| **CP8** | 0.0% | 0.0% | 0.0% |
| **CP9** | 0.0% | 0.0% | 0.0% |
| **CP10** | 0.0% | -0.1% | 0.0% |
| **CP11** | -28.9% | -1.2% | -0.8% |
| **CP12** | 0.0% | -0.1% | 0.0% |
| **CP13** | -28.8% | -1.2% | -0.8% |
| | | | |
| **CPIN1** | -31.6% | -1.6% | -0.9% |
| **CPIN2** | -31.6% | -1.6% | -0.9% |
| **CPIN3** | -0.1% | 0.0% | 0.0% |
| **CPIN4** | 0.0% | 0.0% | 0.0% |
| | | | |
| **CLIN1** | -21.8% | -1.7% | -7.4% |
| **CLIN2** | -21.8% | -1.7% | -7.3% |
| **CLIN3** | -14.8% | -0.4% | -13.2% |
| **CLIN4** | -14.8% | -0.5% | -13.2% |
| **CLIN5** | 0.0% | 0.0% | 0.0% |
| **CLIN6** | 0.0% | 0.0% | 0.0% |

**Table 11.30 Sensitivity analysis result for printer housing**